Stroke on a Chip: Spatial and Temporal Control of Oxygen for *in vitro* Brain Slices

By
Gerardo Mauleon
B.S., University of Illinois at Chicago, Chicago, 2009

THESIS

Submitted as partial fulfillment of the requirements
for the degree of Master of Science in Bioengineering
in the Graduate College of the
University of Illinois at Chicago, 2011.

Chicago, Illinois

Defense Committee

Dr. David Eddington, Chair and Advisor
Dr. Chris Fall
Dr. Thomas Park, Biological Sciences

This thesis is dedicated to my father who has always supported me in all aspects of my life, and my future wife, Jessica, whose constant encouragement helped me get through this project.

ACKNOWLEDGEMENTS

I would like to thank the following individuals for helping me with my research:

Dr. David Eddington - my research and thesis advisor.

Dr. Chris Fall – my research advisor

Dr. Thomas Park - my thesis committee.

Dr. Joe Lo for providing the microfluidic device that allowed long term Fura loading.

Bethany Brown for her assistance during the beginning stages of the project.

My laboratory colleagues for their help and support.

TABLE OF CONTENTS

TABLE OF CONTENTS (continued)

TABLE OF CONTENTS (continued)

LIST OF FIGURES

Figure **Page**

LIST OF ABBREVIATIONS

aCSF	Artificial cerebral spinal fluid
AM	Acetoxymethyl ester
CA	Cornu ammonis
$CaCl_2$	Calcium chloride
ccm	Milliliter per minute (gas flow rate)
CO_2	Carbon dioxide
cm	Centimeter
°C	Degrees Celcius
DG	Dentate gyrus
DMSO	Dimethyl sulfoxide
FOXY	Fluorescent oxygen sensor (Ruthenium-based)
h	Hour
KCl	Potassium chloride
L	Liter
$MgCl_2$	Magnesium chloride
min	Minute
mL	Milliliter
mm	Millimeter
mM	Milimolar
mOsm	miliosmolarity
NaCl	Sodium chloride
Na_2HPO_4	Sodium phosphate dibasic

LIST OF ABBREVIATIONS (continued)

$NaHCO_3$	Sodium bicarbonate
NMDA	N-methyl D-aspartate
μL	Microliter
μm	Micrometer
O_2	Oxygen
PDMS	Polydimethylsiloxane
RPM	Revolutions per minute
s	Second
UV	Ultraviolet

SUMMARY

The hippocampal acute brain slice preparation is an excellent model for studying how neuronal tissue responds to a hypoxic insult, a fundamental question to stroke research. However, current techniques are unable to accurately control the oxygen environment in a way that localized stimuli can be administered. To address this problem, we have developed a microfluidic add-on to a commercially available perfusion chamber that diffuses oxygen throughout a thin membrane and directly to the brain slice. A microchannel is responsible for rapid and efficient oxygen delivery and can be modified to allow different regions of the slice to experience different oxygen stimuli. Using this novel device, we show that we can obtain a stable oxygen environment through out the brain slice and better control over the hypoxic insult as demonstrated with the use of the calcium-indicator Fura-2. Finally, we show that we can independently oxygenate different regions of the hippocampus and measure two independent responses, which is not possible with current techniques.

CHAPTER I: INTRODUCTION AND BACKGROUND

1.1 -The *in vitro* brain slice

1.1.1 -The acute brain slice

Throughout the years, neuroscientists developed several models that have allowed them to study the complexities of the brain in a controlled environment. Models such as dissociated neurons to study the protective effects of drugs (1), or organotypic brain slice cultures to study molecular and electrophysiological responses of neurons have been used (2). However, the acute brain slice preparation is still a preferred *in vitro* model of the brain. Close to half a century ago (3), the acute brain slice preparation, which is used only hours after slicing (4), was introduced to the scientific community in order to provide an *in vitro* model that could offer a way to study the neuronal signaling while still retaining most of the local circuitry (5).

Physiologically speaking, there are several reasons why the acute brain slice preparation is superior to other *in vitro* models. Unlike dissociated neurons, by maintaining the structural integrity, brain slices give researchers an idea of the *in vivo* brain cytoarchitecture, arrangement of the cell bodies. With this, researchers get an idea of the local anatomy and an inside look at the circuitry that the brain has developed (6). Not only that, but by remaining a solid piece of tissue, the slices provide a mechanical stability that allows long-term electrophysiological experiments. In addition to the mechanical stability, brain slices are able to provide experimental stability that cannot be obtained during *in vivo* experiments; one of the weaknesses of the *in vitro* model actually becomes one of the strengths. Thanks to the absence of a heartbeat and pulmonary movement, which would lead to pulsations; long-term electrophysiological experiments are possible (7). Also, pharmacological experiments can be performed without having to worry about the blood-brain barrier (7). In short, all metabolic and vascular influences

are mostly absent, which allows researchers to study the effect of certain stimulants in isolation (8). Like all *in vitro* models, the local environment is easily controlled, so the researcher can manipulate the oxygen concentration, carbon dioxide, pH, temperature, and ion concentration (5). Finally, one advantage of brain slices over *in vivo* models that cannot be undermined is the accessibility afforded by the slice. By doing *in vitro* experiments, the researcher can easily visualize the area of interest and can accurately place electrodes, apply chemicals, or move the tissue in whatever form is needed to improve the chances of success; something that cannot be done *in vivo* (9).

1.1.2 -The hippocampus

The hippocampal acute brain slice preparation, with its defined cytoarchitecture, mechanical stability, and recognized sensitivity to oxygen variations (10, 11), provides an *in vitro* model where the spatio-temporal effect of oxygen on neuronal tissue can be isolated from any other variables.

The hippocampus's role in memory formation and the fact that it is particularly sensitive to oxygen level changes are well documented (12, 13, 14). The hippocampus is divided in several areas depending on what types of cells are present in such area; for example, granular cells populate the dentate gyrus while the 4 "CA" areas are full of pyramidal cells (15, 16). From the different areas of the hippocampus, the CA1 area is the most vulnerable to hypoxic events, followed by the dentate gyrus, which also suffers neuronal damage (16).

The oxygen variations of the hippocampus are hard to study on live animals, which is why the *in vitro* preparation is preferred for hippocampal studies (17). The animals studied in

this project were mice 17 to 21 days post-natal since this age group presents an ideal balance between resistance to hypoxia and ease of dye loading (18).

1.1.3 -Hypoxia and calcium

During the process of this project, one of the factors studied was the correlation between hypoxia and calcium ions inside of the cells. As previously mentioned, the brain and all of its functions are highly regulated by the oxygen supply and anytime there is a change in the oxygen's concentration, the tissue will show the effects (14). It is currently known that a drop in oxygen concentration can lead to energy failure and eventually cell death through a series of parallel and complex mechanisms that are still studied today (16). One of the first consequences of hypoxia in the neurons is the markedly decrease in the ATP production, which is necessary to maintain the cellular membrane integrity (19). As soon as the cell membrane starts to malfunction, a series of ionic changes occurs inside the cell, which ultimately lead to the cell dying; some of the most important ionic disturbances include sodium, hydrogen and calcium (14).

A period of hypoxia starts a chain of events that can eventually lead to cell death. Even though the exact mechanism by which this occurs is not completely understood, there are several theories that attempt to explain this whole process. In fact, the accepted truth is that many different mechanisms work parallel to each other to elevate the intracellular calcium levels. For the most part, these mechanisms involve voltage-gated calcium channels, neurotransmitters binding to glutamate receptors, calcium/sodium exchange during cell depolarization, and release of intracellular storage of calcium (19). Several reports indicate that whenever the ATP of the cell is depleted, the cell depolarizes and allows extracellular calcium to enter the cell throughout

voltage-gated calcium channels (20, 21). Also, another reason why the intracellular calcium increases inside the cell during a hypoxic insult is that it comes from within. Several studies show that some of the organelles inside the cell release their calcium contents (1, 22), the largest calcium reservoirs inside the cell belong to the mitochondria and the endoplasmic reticulum (21, 23). However, most current models agree that even though the previous methods have an effect on the intracellular calcium increase, the main factor corresponds to an influx of calcium due to a great release of glutamate from the cells (11).

As with everything in the body, a firm balance between the intracellular and the extracellular calcium concentrations is kept thanks to the cellular membrane. Only when certain channels, located on the plasma membrane, are activated, can the calcium ions flow into the cell effectively depolarizing the cell. One of these receptors is the N-methyl D-aspartate (NMDA) receptor, which is a subclass of glutamate receptors, an excitatory amino acid. These NMDA receptors act as the activation switch for cation channels that calcium ions are specially favored to use (11). If a glutamate molecule is able to find the receptor's binding site, then the channel will open allowing calcium a way into the cell.

However, during a hypoxic period, several things occur that are out of the ordinary. First, during the state of hypoxia, the binding force of the NMDA receptors increases drastically effectively leaving the channels open for a longer amount of time (1). Also, the glutamate neurotransmitter is released in massive quantities into the extracellular space and these high concentrations over activate all of the glutamate receptors, leading to a condition know as excitotoxicity, because of the excitatory glutamate neurotransmitter's actions (16). Even though the NMDA is the principal contributor to the increase of calcium, especially because of its high permeability to calcium, there are other receptors that work in this process. For example, the

activation of AMPA subtype of glutamate receptors is also accepted as a way in which the calcium increases and causes a cell depolarization that leads to an enhance in the activity of the NMDA channels (19). Several other peptides also cause glutamate to increase in concentration in the extracellular space and cause depolarizations (24). In the end, no matter what the mechanisms are, the result is the same; excitotoxicity: overactivation of glutamate receptors causes an increase in the intracellular calcium leading to cell depolarization and cell death (24, 25).

The exact process by which the calcium ions cause the cell to die is also not entirely understood. Calcium is one of the most important second messengers in the body. It is involved in muscle contraction, cell division, and signal transduction in the brain via neurotransmitter release in the presynaptic neuron or direct activation of receptors in the postsynaptic neurons (1). How this ion leads to neuronal death is a great mystery, however, for over thirty years now, scientists have shown evidence that an increase in the intracellular calcium of the cell is toxic for the cell and results in injury and ultimately death for the cells (10, 21). Even though the exact mechanism is still missing pieces, the proposed mechanisms include the activation of calcium dependent lipases, nucleases, proteases, etc., not to mention damage to the metabolism of the cytoskeleton and also the cell membrane (19). However, if the environment goes returns to normal before it is too late, the membrane can repolarize and return to homeostasis by pumping out the calcium ions (25).

1.1.4 -Fura-2

Now that the importance of intracellular calcium has been established, it is necessary to study the relationship between hypoxia and calcium. Using synthetic molecules that bind to calcium ions, it is possible to indirectly measure the intracellular calcium concentrations (26).

Since 1985, the Fura-2 molecule has been used to as a tool to image neuronal populations in an attempt to further decipher the cell's circuitry (27). Fura-2, when combined with the acetoxymethyl ester (AM) group is able to penetrate the cell membrane of the neurons and bind with the free calcium ions present in the vicinity (28). There were other methods used to measure the intracellular calcium before the invention of the Fura-2 molecule; however, the advantages provided by this molecule are too great to ignore. First of all, the Fura-2 molecule has the innate ability to change its excitation wavelength whenever a calcium ion binds to the molecule. Using what is now called ratiometric imaging, the calcium concentrations can be measured using the ratio of 340 and 380nm (29). Thanks to ratiometric imaging, it is possible to almost negate several experimental errors, such as instrument efficiency, the final concentration of the fluoresent dye, any leakage present, and most importantly, photobleaching (30).

By using the Fura-2 molecule, studies about the intracellular calcium concentrations of the neurons are possible. First, the cell is loaded with the Fura-2/AM complex, and then once the loading is done, the cells can be exposed to an excitation wavelength of 340nm followed by the 380nm wavelength. After this, the dye will emit a 505nm wavelength that can be picked up with the microscope. During the experiments, the signal will be constant as long as the cell's environment is constant, however, when the hypoxic insult is applied and the calcium ions flow into the cell, they will bind to the Fura-2 molecule; at this point, the molecule will shift its

wavelength to a lower intensity one which will be apparent in the computer. This dip in the signal will signify the influx of calcium ions.

1.2 –Current hypoxic techniques

1.2.1 –Perfusion

As the years passed, and researchers realized the potential that the acute brain slice preparation had, several methods have surfaced in an attempt to take full advantage of the slices. For the most part, most of the experiments rely on perfusion of the slice with a liquid that mimics the intact brain. The experiments are usually carried out on devices called perfusion chambers, which allow the slices to remain viable for several hours (9). Most of these chambers are a variation of the Haas perfusion chambers (31), and as such, are mostly intended to work with upright microscopes and top-based electrophysiological tools (6, 31). Originally, these chambers consisted of a chamber with a nylon mesh secured at a predetermined elevation. This way, the slice could be placed in this mesh and be oxygenated from 2 sides. The topside was exposed to humidified air while the bottom of the slice was exposed to the oxygenated perfusion. These initial recording chambers are in a class now called interface-type chambers (32). Finally, in an attempt to immobilize the slice, a metal mesh, called a harp, can be placed on top of the slice (33).

With the slice immobilized and exposed to the perfusate, researchers realized that the perfusion should mimic the cerebral spinal fluid as much as possible. In order to do this, artificial cerebral spinal fluid (aCSF) is bubbled with 95% oxygen in order to fully oxygenate the slice, and the ionic composition of the liquid is tightly regulated (3). Finally, different drugs can be dissolved in the aCSF in an attempt to recreate a natural signal response from the brain (34). Of

course, since all of these experiments need the slice to be exposed to the aCSF, then the flow rate is carefully monitored. A higher flow rate would accelerate the drug reaction and bring more oxygen to the slice, which is diffusion limited. However, a higher flow rate would also lead to mechanical instability due to the shear stress experienced by the slice, which would hamper electrophysiological and imaging studies (32).

Even though chemicals can be dissolved into the perfusate to mimic a brain reaction, neuroscientists have also tried applying the drug to only a small area of the brain. In order to perform these local experiments, local microinjections using tools such as micropipettes have been used (33). Also, capillaries can be placed on top of the slice whenever patch-clamping recordings are needed (6). Overall, many type of studies are possible with the perfusion chambers used so far; however, capillaries and micropipettes can become tedious if more than one is needed to perform the necessary studies.

As previously mentioned, experiments are currently performed with perfusion chambers that flow aCSF that is bubbled with 95% oxygen in order to fully oxygenate the slice. Thanks to these methods, the brain slices are able to stay viable for up to 8 hours; however, whenever hypoxic insults are performed; their implementation is not ideal. Currently, a change in the perfusing medium is used in order to change the oxygen levels of the slice or sometimes glass micropipettes are used to inject soluble chemicals into the extra and intracellular medium to provoke a stroke (8).

1.2.2 –Perfusion chamber types

Over the years, several types of perfusion chambers have been designed. Even though there are several styles and each one has several advantages over the rest, all of them can be classified in one of two groups: interface- and submerged-type chambers.

In interface-type chambers, a nylon mesh is placed in the chamber in such a way that the slice is slightly elevated from the bottom of the chamber. By doing this, the perfusate can deliver nutrients and oxygen to the bottom of the slice while the top face is exposed to a humidified gas (32). Because of the type of tools used for neurophysiology experiments, this type of chamber has proven highly reliable and is a staple of many studies (34).

On the other hand, in submerged-type chambers, as the name implies, the slice is completely covered by the perfusate and due to this, there are several advantages. Not only do these chambers offer the capacity of improved imaging techniques, but they also allow drugs dissolved in the aCSF to take effect faster than in other types of perfusion chambers (34). However, in both, the interface-type and the submerged-type chambers, gradients of both oxygen and chemicals are created.

1.2.3 –Flaws of the perfusion method

Now, while the invention of the perfusion chamber has allowed neuroscientists to learn much knowledge about the details of how the brain behaves and interacts within itself, the perfusion method is not perfect. Neuroscientists discovered long ago that the brain, and for that matter all organs and tissues, do not need a global stimulus to create a response. Using current techniques, the brain slices can be exposed to a chemical through the perfusing medium (which bathes the whole slice), or exposed to a hypoxic insult (which again affects the whole slice).

Sometimes only a small area of the brain is studied and yet the whole slice is disturbed; such experimental protocols can potentially lead to misguided results. More realistic experimental conditions are necessary in order to gain full understanding of the brain pathways. In order to achieve a higher understanding of brain dynamics, spatially controlled stimuli, which are temporally controlled, should be created, this way the brain could be exposed at several sites and the dynamics of it could be better understood.

One of the biggest drawbacks of using the brain slice preparation is the need to rely on diffusion for nutrient and oxygen supply. Even though in the intact brain, diffusion is also used to deliver the necessary nutrients, the distance that the blood must travel is only as thick as the capillaries themselves, that is, only 30-60μm (35). Also, while in the brain, the blood oxygen levels in the arteries are roughly 90mm Hg, while inside the brain tissue these values drop to 20 to 5 mm Hg (35). It should come to no surprise that the oxygen levels on the brain are highly regulated. Due to its role in several signaling pathways, the brain is extremely sensitive to oxygen levels and any change in these levels has a great impact on the brain functions (36, 37, 38). As such, the oxygen levels in the perfusing fluid are continually controlled in order to maximize the diffusion of oxygen into the tissue.

However, since the delivery of oxygen depends on it diffusing through a thick layer of cells- somewhere between 200 and 400μm for most experiments-, parts of the tissue do not get the oxygen supplies that it needs. In fact, several studies have confirmed that the parts farthest away from the oxygen supply (the core in the interface-type and the bottom in the submerged-type chambers) are lacking oxygen (17, 39). The lack of oxygen can quickly lead to necrosis and eventually death of the cells (37).

Cell death due to an absence of oxygen is the final step during a stroke. In an effort to understand more about the effect of hypoxia on the neuronal cells, several studies have induced hypoxic insults on brain slices using the perfusion method. The ability to induce a hypoxic insult that better mimics the effects of a stroke should provide researchers a better tool for stroke research.

1.3 –Microfluidics

1.3.1 –Polydimethylsiloxane (PDMS)

The polydimethylsiloxane (PDMS) polymer has several important properties that are beneficial to the biological community. For example, the PDMS components have a very low glass transition temperature, and as such, they are in the liquid state at room temperature and can be cross-linked with heat; once it is polymerized, PDMS is relatively elastic depending on the curing agent, cross linker ratio used (40). Another reason why PDMS makes an ideal platform for biological experiments is because it is optically transparent and has a surface that is not only hydrophobic and chemically stable, but is also nontoxic and can be sterilized by many conventional methods (33, 36). Also, even though this material is inherently hydrophobic, with the application of a plasma treatment, the surface can become hydrophilic making it easier to perform experiments (41). Another reason why PDMS is a material of choice for many biological applications relates to the ability to mass-produce PDMS devices. Thanks to this ease of fabrication, the PDMS devices can be produced relatively fast and be optimized to the experimental needs (33). Finally, PDMS is an optimal material for biological experiments due to its high oxygen diffusivity, which is in the same order as water, to nonpolar gasses, mainly

oxygen (42, 43). If the PDMS layers are small enough, it is safe to assume that the gasses will diffuse across the layer to fully oxygenate the biological tissue on the other side (42).

As previously mentioned, PDMS is one of the main polymers used in microfabrication (41). This polymer is sold in its unpolymerized form. To make it, the silicon base (vinyl-terminated PDMS) and the curing agent (mixture of platinum complex and copolymers of methylhydrosilane and dimethylsiloxane) are mixed in a predetermined ratio (usually 10:1) and degassed. After this, the mix can be poured over a mold and heated to about 85 degrees Celsius at which point it solidifies thanks to the hydrosilylation reaction of the vinyl groups and the hydrosilane groups (44), this is a cross-linked elastomer.

1.3.2 –Soft-lithography

Microfluidics is a field that originated as a result of the advances in microfabrication, most importantly thanks to the development of photolithography. With this technology, devices with structures as small as 250nm were possible to fabricate (44), however, their role in biological experiments was limited due to the fact that this technology can be expensive, it is hard to modify the surface of the device to accommodate for cells and proteins, and can only be produced on photoresists (41).

In order to bring the advantages of microfabrication to the biological community, soft-lithography was created. Soft-lithography gets its name from the fact that an elastomer is used as a mold to create the micro-sized structures (40). With this new invention, the biological community, including neuroscience, has started to take advantage of this technology (2). Soft-lithography is a cheap technique when compared to photolithography and is capable of creating features as small as 1μm. From a SU-8 patterned silicon wafer, a PDMS chip is created which

can then be used many times over (2). One of the main things about this technique involve the use of elastomeric materials, such as PDMS, to create devices that have a patterned structure on their surfaces (44), this is done via a technique called replica molding.

In this process, a master is made using photolithography techniques. SU-8 (a photosensitive epoxy) is first poured over a silicone wafer, and then a mask with a predetermined design is placed on top of the wafer and exposed to UV light. The UV light will polymerize the exposed epoxy areas and any unpolymerized epoxy will be washed off. In the end, the master will have a raised design that will be a negative of the final wanted design (40). In order to maximize the master's efficacy, a process called silanization can be applied to the master; in this process, the chemical silane (in vapor form) is deposited on top of the master for a period of two hours (45).

After this step, the PDMS mold is made thanks to cast molding. In cast molding, the polymer mix (a combination of prepolymer and curing agent) is poured over the master and heated up. By doing this, the polymer mix polymerizes and solidifies. After this, the PDMS block can be lifted up from the master and in one hand you have a PDMS device with a patterned structure and on the other hand you are left with a master than can be reused many times over (40).

1.4 –Research purpose

For our study, we combine the ideas of modifying a perfusion chamber to control the spatio-temporal delivery of stimuli with an improved oxygen delivery method. We designed and engineered a microfluidic add-on to a commercially available perfusion chamber that diffuses oxygen throughout a thin membrane and directly to the brain slice. A microchannel is

responsible for the rapid and efficient oxygen delivery and can be modified to allow different regions of the slice to experience different oxygen stimuli. Using this novel device, we can achieve a more stable oxygen environment throughout the brain slice, and attain better control over the hypoxic insult as demonstrated with the use of the calcium-indicator Fura-2. Finally, we show that we can independently oxygenate different regions of the hippocampus and measure two independent responses demonstrating the utility to stroke research.

CHAPTER II: Materials and Methods

2.1 –Device fabrication

During the process of this project, a microfluidic device was used to manipulate the oxygen environment experienced by the brain slices. In order to accomplish this task, different versions of the same basic approach were designed. As described in the introduction, the devices were fabricated with similar methods with the microchannel being the main difference between devices. The microfluidic channel and the membrane were fabricated out of the elastomer PDMS using soft lithography. Alignment marks were used to create holes in the PDMS membrane and in the perfusion chamber in such a way that they allowed the oxygen to flow into and out of the microfluidic channel. Once the individual parts were aligned, they were irreversibly bonded to complete the device. The perfusion chamber allows the slice to be completely submerged under the aCSF while the PDMS membrane provides a mechanically stable surface for the tissue. The optically transparent PDMS allows clear visualization of the neurons from the bottom of the device, which is necessary to measure changes in fluorescence intensity observed with the calcium indicator. Also, since we are modifying an open bath perfusion chamber, the top of the device allows the use of most applicable neuroscience tools.

The devices main difference lies in the microchannel responsible for delivering the oxygen. The two designs mainly used during the process of this project are shown in figures 2.1.A. While the single channel design main focus was to provide temporal control, the multiple channels design also provides spatial control over the oxygen environment. Advances in microfabrication techniques allow the customization of microfluidic devices in a short amount of time. The multiple channels design is essentially identical to the single channel design except

that instead of one microfluidic channel supplying the oxygen to the entire brain slice, several independent microchannels can supply different regions of the slice with different oxygen concentrations. Just like the previous device, the device using this design is an addition to the common perfusion chamber (Warner Instruments, RC-26GPL) shown in figure 2.1.B. The walls dividing each individual channel are 0.3mm wide and allow complete oxygen independence from one channel to the next. The design of this device allows the hippocampal region to be divided in 2 sections: the CA1 area can be placed on top of one channel, while the dentate gyrus can be placed on a separate channel.

A)

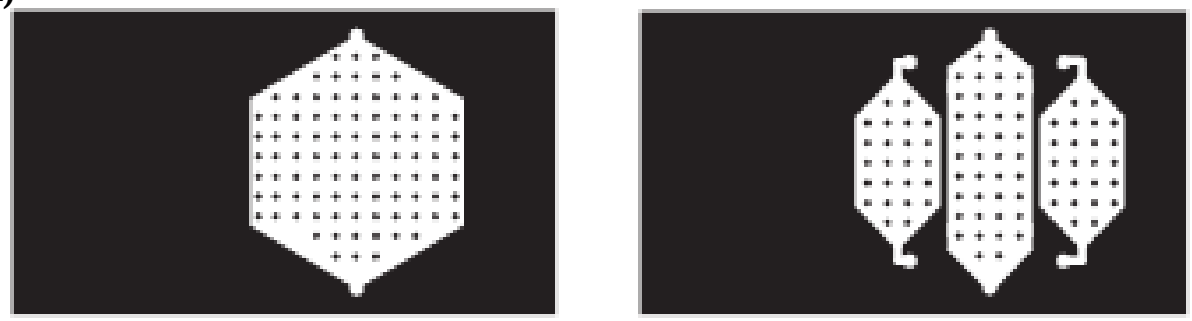

B)

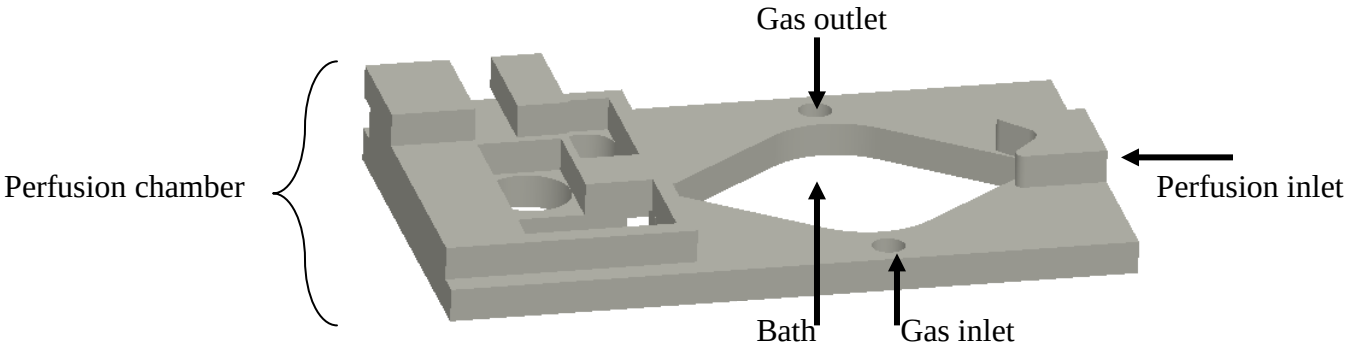

Fig. 2.1. Photomasks and perfusion chamber. A) Photomask's designs used for fabrication of the microchannels of the device. Both the single channel and the multiple channels designs allow oxygen to flow through them and then diffuse into the tissue. B) Standard perfusion chamber (RC-26GLP). Two holes were drilled at predetermined positions in order to act as the gas inlet and outlet.

2.1.1 –Microchannel component fabrication

The photomask design was created in Adobe Illustrator CS4 and printed onto high resolution (16,000 dpi) transparency film (Fineline Imaging). To fabricate the negative mold master, a 3-inch silicon wafer (Silicon Sense) was thoroughly cleaned before being centered on the mounting block of a precision spinner (Laurel) with the aid of a wafer-centering tool and subsequent manipulation if necessary. Figure 2.2 outlines the major steps taken during this fabrication process.

SU-8 2150 photoresist (MicroChem Corporation) was the photoresist chosen in this case in order to achieve the desired thickness of 200 µm. The SU-8 was slowly poured on top of the wafer until it had covered about two thirds of the surface of the wafer. In order to achieve the desired thickness, the wafer was spun to an initial spin velocity of 500 rpm for 10 seconds, followed by a spin velocity of 1900 rpm for 30 seconds.

Following the spinning cycle, a baking step, so called soft-bake, must be performed. In order to perform this step, the wafer was carefully removed from the spinner and then placed on a leveled hot plate set to 65 °C for 6 minutes. After this time, the wafer was removed from this first hot plate and placed in a second hot plate set to 95 °C and baked for 39 minutes. This is a necessary step in order to evaporate the SU-8 solvent. After the allotted time, the wafer was removed and allowed to cool to room temperature before the next step took place.

As can be seen from figure 2.2, the next step in the microfabrication process is called UV exposure. During this step, the wafer will be selectively exposed to UV light, which will polymerize the exposed SU-8 regions. In accordance to safety protocols, this process was done while using UV protecting glasses in order to prevent retinal damage from the UV light. Before exposing the SU-8-coated wafer to UV light, the UV lamp's output intensity was measured using

a radiometer (Exfo R2000). The UV lamp output must be measured before each exposure in order to make sure that the proper energy is released from the lamp, as the UV source will lose intensity over time. Once the energy output was measured, the lenses of the system were properly set up. The wafer is then placed on a predetermined spot, with the photomask transparency placed directly on top of it, as well as the quartz glass disc the same diameter as the wafer that is also placed on top of the wafer. After making sure that the energy beam covered the entire surface area of the wafer, the wafer is exposed to UV light to selectively polymerize the SU-8. In order to achieve the desired thickness of 200 μm, the photoresist was exposed to 315 mJ/cm^2 of UV light. The exposure duration was calculated using the following formula:

$$Exposure\ Duration = \frac{Energy\ Density}{\left(\frac{Lamp\ Output}{S.A.}\right)} \tag{2.1}$$

where the energy density is obtained from the SU-8 manufactorer, S.A. represents the surface area of the wafer (45.6 cm^2), and the lamp output is the value measured with the radiometer.

After exposing the photoresist, the next step is called post-exposure bake. In this step, the wafer is placed back onto a hot plate set to 65 °C for 5 minutes and then in one set to 95 °C for 14 minutes. After the allotted time, the wafer is allowed to cool to room temperature.

Finally, any uncross-linked regions of the photoresist were removed by washing the wafer in SU-8 developer solution. To remove any unexposed regions of the resist, used developing solution was initially used. The wafer was placed on a flask that could hold about 5ml of developing solution and then it was agitated for about 20 minutes. After this time, the wafer was washed with isopropanol and then dried under nitrogen gas. After drying, the used

developer solution was replaced with new developing solution to effectively clean the photoresist. The wafer was agitated in this new bath for about 3 minutes and then it was rinsed once again and dried again.

Once the SU-8 negative master was fabricated, it was subjected to a chemical procedure called silanization. To perform this process, 30µl of silane solution, Tridecafluoro-1, 1,2,2-TetraHydro Octyl-1-Tricholosilane (UCT Specialties), were deposited on a 5ml beaker and placed on a vacuum chamber, then, the master was placed in this same chamber and a vacuum was created. During this process, the silane solution was vaporized and a small layer of silane was deposited on the master. Thanks to this layer, other chemicals do not stick as strongly to the master and they will be easier to peel off (45). Following safety protocols, this process was done inside of the fume hood in order to prevent toxic gases from going into the lab space. The silanization process lasted for 2 hours.

To fabricate the positive mold of the microchannel, 2 batches of about 5 grams of PDMS were prepared in a 10:1 mixture of prepolymer and curing agent (Sylgard 184 kit, Dow Corning); mixing lasted for about 5 minutes with extensive bubbles being a reasonable indicator of liquid homogeneity. The PDMS mix was then degassed in a desiccator (Adixen, Pascal 2010 SD) to remove the bubbles. Once the bubbles were gone, the PDMS was spin-coated onto the master. The PDMS spinning protocol is very similar to the SU-8 spinning protocol. As such, the master was placed in the spinner and one of the batches of PDMS was poured on top of the wafer. In order to achieve a thickness of 200µm, the wafer was spun twice. The PDMS was first poured and spun initially at 500 rpm, followed by a spin velocity of 800 rpm for 30 seconds, after this, the master was baked for 15 minutes at 75°C in a hot plate. After this baking time, the master is again placed in the spinner and the second batch of PDMS is spin-coated on top of the master at

the same speed followed by curing for 2 hours at 75°C; this combined process creates a 200μm thick PDMS layer. We made sure to remove any and all bubbles that formed during the spinning or baking process, especially bubbles formed at the holes of the microchannels. In the end, these holes will become the support pillars, and if a bubble forms here, a pillar will not formed. In order to remove the bubbles, the wafer was placed in a high strength vacuum for about 2 minutes, during which time the bubbles came out of the holes and disappeared.

Once the PDMS cured, the microchannels were peeled off the master. This is a very delicate process since even a small rip in the microchannel could destroy the entire device. In order to successfully peel the microchannel off of the master, a thin-tip blade was used to cut the PDMS along the alignment marks. Then, a dentist probe was used to lightly separate most of the microfluidic channel area from the master itself, making sure not to rip the PDMS device. Finally, using 2 small-tip tweezers, the microchannels were slowly peeled off from the master taking special care to remove the support pillars without breaking them.

One advantage of the device design is the ability to generate complex spatial oxygen profiles, dependent upon the microchannel. During the duration of this project, several different microchannel designs were fabricated in an attempt to enhance the device's utility. The first design used consisted of a single microchannel that allowed a uniform oxygen concentration. However, during the latter parts of the project, the designs consisted of multiple microchannels that provided spatial control to the microfluidic device.

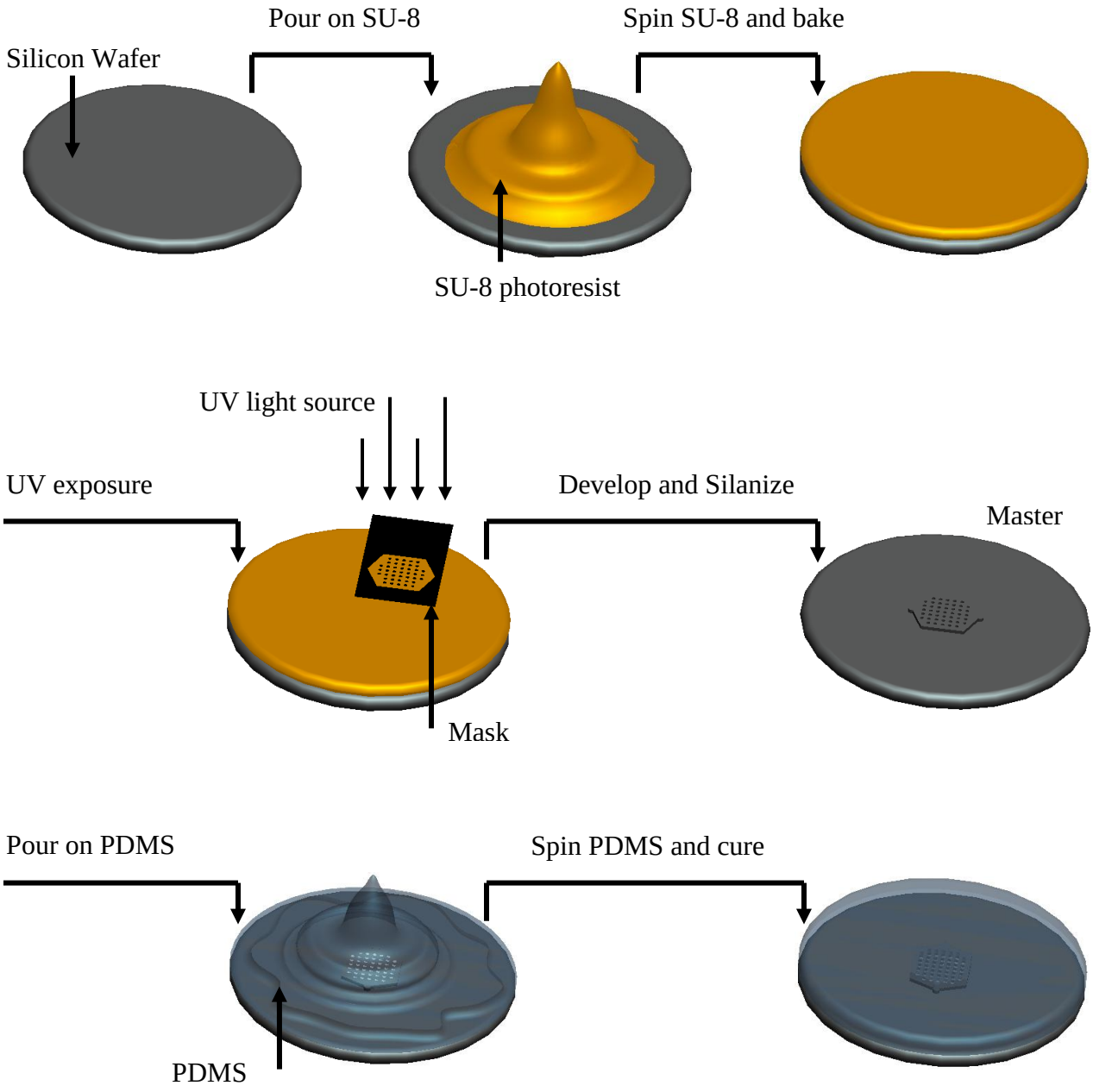

Fig. 2.2. Schematic of the master mold and the PDMS device fabrication. SU-8 2150 photoresist is spin-coated onto a silicon wafer, and selectively exposed to UV light through a photomask. After this step, the exposed wafer is developed and silanized producing a reusable master. PDMS is then spin-coated into the master and allowed to polymerize. The PDMS mold can then be peeled off from the master.

2.1.2 –Membrane fabrication

In order to make the 100µm-thick gas-permeable membrane, a process similar to the microchannel fabrication was used. 5 grams of PDMS were mixed in a 10:1 mixture of prepolymer and curing agent as previously mentioned. Next, a thoroughly cleaned 3-inch silicon wafer was placed on the spinner and the PDMS mixture was poured over the wafer until it covered about two-thirds of the surface area of the wafer. After this, the PDMS was spin-coated onto the wafer using a speed of 500 RPM for 10 seconds followed with a speed of 800 RPM for 30 seconds in order to achieve the desired thickness of 100µm.

Once the spinning cycle was done, the PDMS-coated wafer was transferred to a hot plate set to a temperature of 75°C for 2 hours. Once the PDMS layer was cured, a section equal in size to the microchannel component was cut using a thin-tip knife. Then, using a dental probe and tweezers, the PDMS membrane was peeled off from the wafer and placed on a transparency film in order to facilitate handling.

Following this step, using the microchannels as an alignment mark, small holes that would work as the inlet and outlet ports were made in the membrane using a blunted punch hole. This is a very important step in the fabrication process as these holes will allow the gas into the microchannels and if the holes do not align with the inlet and outlet of the microchannels, then the device will not work as expected.

2.1.3 –Perfusion chamber modification

A standard off-the-shelf perfusion chamber (RC-26GPL, Warner Instruments) was used for this project. Using the microchannel component as reference, inlet and outlet ports were

drilled in opposite sides of the perfusion chamber. The finalized holes have a circumference of 1.5 mm and were finely polished in an effort to maximize gas flow.

The perfusion chamber was used because one of the goals of this project is to maximize propagation of this new technology. Researchers in neuroscience, not necessarily familiar with microfluidic technology, are prime candidates to take advantage of this new tool and by merely modifying a currently used tool in the field, it is expected that its use will increase.

2.1.4 –Device assembly

Once the gas-permeable membrane, the microchannel component, and the perfusion chamber were completed, the device was ready to be assembled. This process was completed in 2 steps both of which used surface plasma treatment for PDMS bonding. During this plasma treatment, the PDMS is slightly decomposed creating free radicals that can then cross-link with other surfaces creating an irreversible bond between the device's layers. The overall process is highlighted in figure 2.3.

First, the gas-permeable membrane and the microchannel component were bonded together. To do this, the surfaces to be bonded together were first dabbed with Scotch tape in order to remove any particulates such as dust. Then, the surfaces were exposed to oxygen plasma using an air plasma handheld wand (BD-20; ElectroTechnic Products) for about 1 minute on each component. Then, the membrane is placed on top of the microchannel making sure to align the inlet and outlet of the microchannel with the holes in the membrane and also ensuring that the membrane is making a flat surface with the microchannel. After this bonding process, the PDMS device is incubated at 75°C for 2 hours to completely finish the bonding process.

Once the PDMS device was finished, it had to be docked into the perfusion chamber. To do this, a light coating of mixed PDMS, again in a 10:1 mixture of prepolymer and curing agent, was applied to the bottom of the chamber and allowed to partially cure in a hot plate set to 75°C for 15 minutes. Then, the PDMS device and the PDMS-coated chamber were exposed to oxygen plasma in their respective bonding surfaces as previously mentioned. The chamber was then placed right on top of the PDMS device making sure to align the inlet and outlet ports of the chamber with the holes in the PDMS device. After this, the completed device was incubated at 75°C for 2 hours. The oxygen plasma exposure helps to create a watertight seal that allows the chamber to be fill with aCSF without leaking. The finalized microfluidic device is shown in figure 2.4A and figure 2.4B shows a schematic of how the oxygen travels through the device.

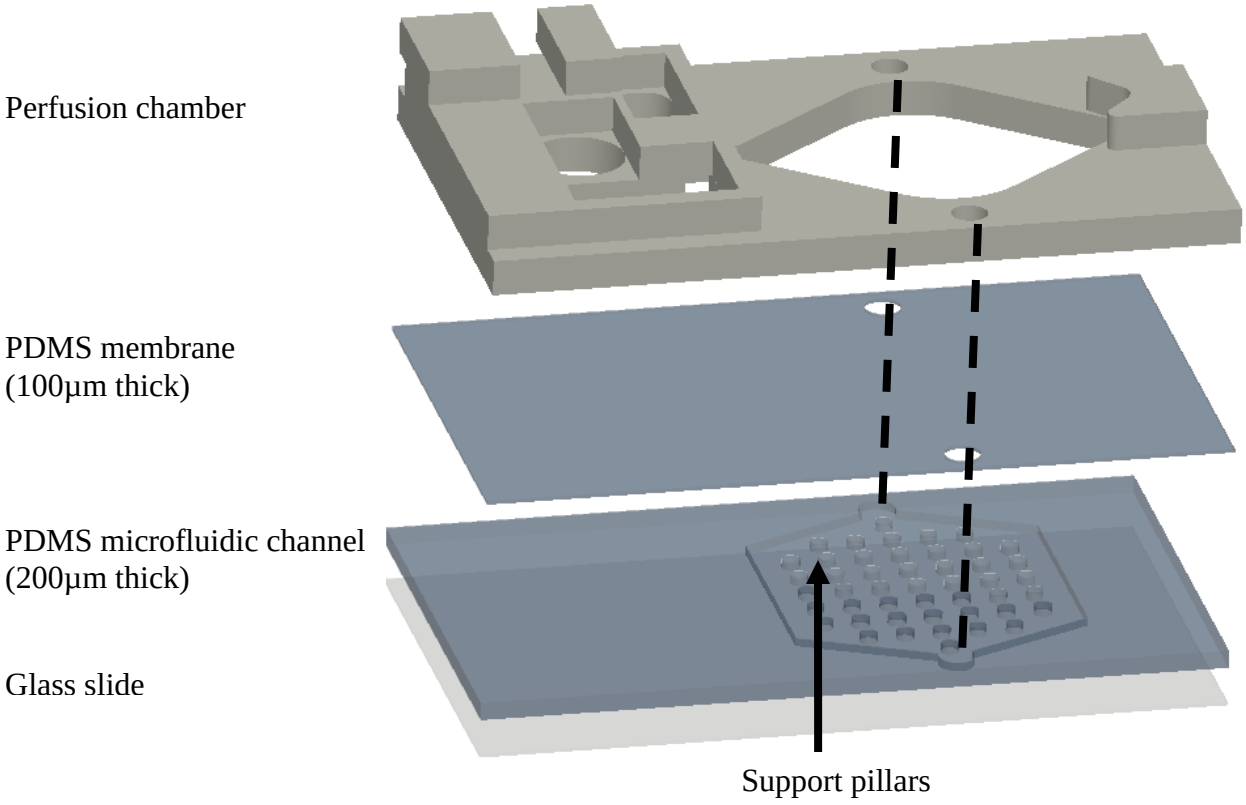

Fig. 2.3. Schematic of the microfluidic device. A) Exploded view of the microfluidic device. As seen from the diagram, the device consists of 4 independent parts: the perfusion chamber, the PDMS membrane, the PDMS microfluidic channel, and a glass slide. Alignment marks show how the gas is supplied to the device.

A)

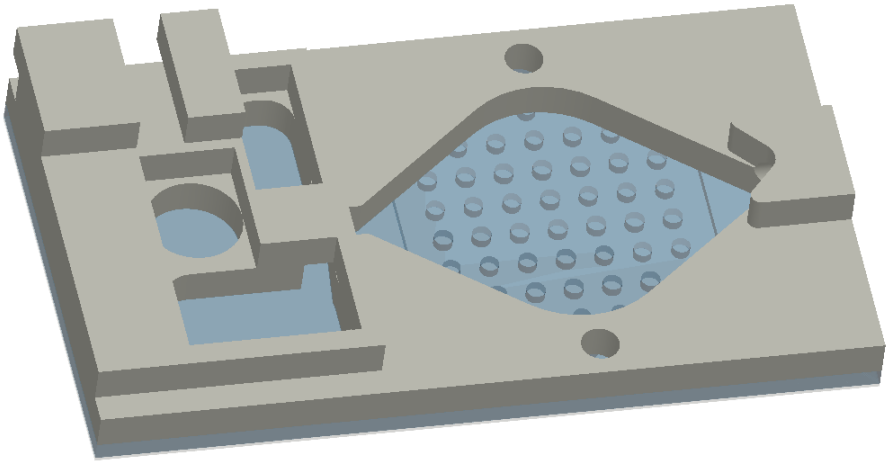

B)

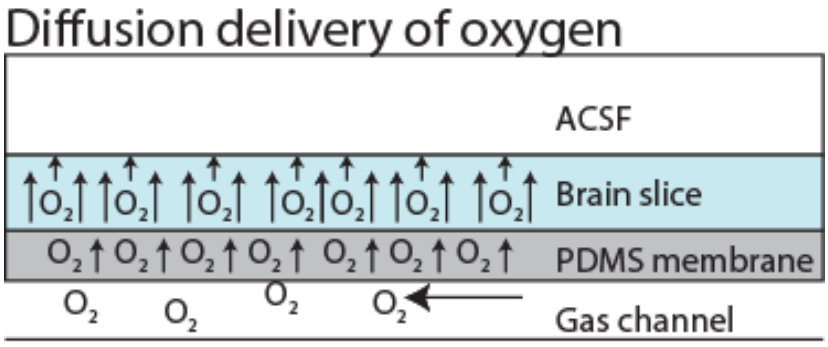

Fig. 2.4. Finalized device and schematic of oxygen diffusion. A) Picture showing the completed device. Oxygen plasma allows the PDMS components to bond to the perfusion chamber. Once finalized, the device can be filled with aCSF. B) Schematic showing how the microfluidic device works. The microchannel is filled with oxygen gas, which can then travel across the PDMS membrane and alter the oxygen environment of the brain slice or the aCSF.

2.2 - Oxygen concentration validation measurements

A hand held oxygen sensor was used to measure the oxygen delivered by the device to where the tissue would be positioned. Oxygen measurements were taken with and without tissue as the oxygen inside the tissue is a very good indicator of the efficiency of the device. Figure 2.5 shows the oxygen validating system, showing the hand-held probe and the software.

2.2.1 –Oxygen concentration in aCSF as a result of the microfluidic device

2.2.1.1 –Hand held oxygen sensor

A hand-held optical sensor (Neofox, Ocean optics) was used to determine the oxygen concentration inside and outside the brain slice. This is a fluorescent-based optical oxygen sensor that is composed of 2 main parts: the fiber optic probe (Foxy-PI200, Ocean Optics) and the oxygen sensing system software (Neofox).

In order to work, this system must first be calibrated according to the manufacture's instructions. Namely, the probe is exposed to gas containing 0% O_2 (95% N_2/ 5% CO_2) for 30 seconds, followed by gas containing 95% O_2 (95% O_2/ 5% CO_2) for 30 seconds. Once calibrated, the probe will be able to determine the oxygen concentration in any environment, gaseous, liquid, or solid.

2.2.1.2 –Gas infusion system

As was previously mentioned before, the microfluidic device used in this project works thanks to the combination of the microchannel and the PDMS membrane. If the required gas concentration is supplied at the correct flow rate, then the gas will be able to propagate through the microchannel and diffuse throughout the PDMS membrane into the brain tissue without

disturbing any imaging process. In order to supply the gas contents to the microfluidic device, a customized system was developed as shown in figure 2.6.

It is important to remember that the correct flow rate is necessary in order to obtain adequate results. If the flow rate were slower than necessary, then the diffusion time into the environment would increase. On the other hand, if the flow rate were too fast, then the PDMS membrane would bulge and in the worst case-scenario, tear the membrane completely.

Gas tanks containing the required oxygen concentrations were purchased from Air Gas as well as its respective top regulator. To control the flow rate of the gas, a flow rotometer (Omega; FL-5511G) was attached to the top regulator using large diameter tubing (Cole-Parmer; EW-06429-36) and metal adapters. Then, the rotometer was connected to a 3-way stopcock (Cole Parmer; EW-30600) using small diameter tubing (Watson Marlow). The 3-way stopcock was used to easily switch between one gas concentration to the next and to divert the gas flow for the multi-channel experiments. Finally, the stopcocks used the same small diameter tubing to connect to the microfluidic device. In the end, the oxygen gas was supplied at a rate of 38ccm to the microfluidic gas channel.

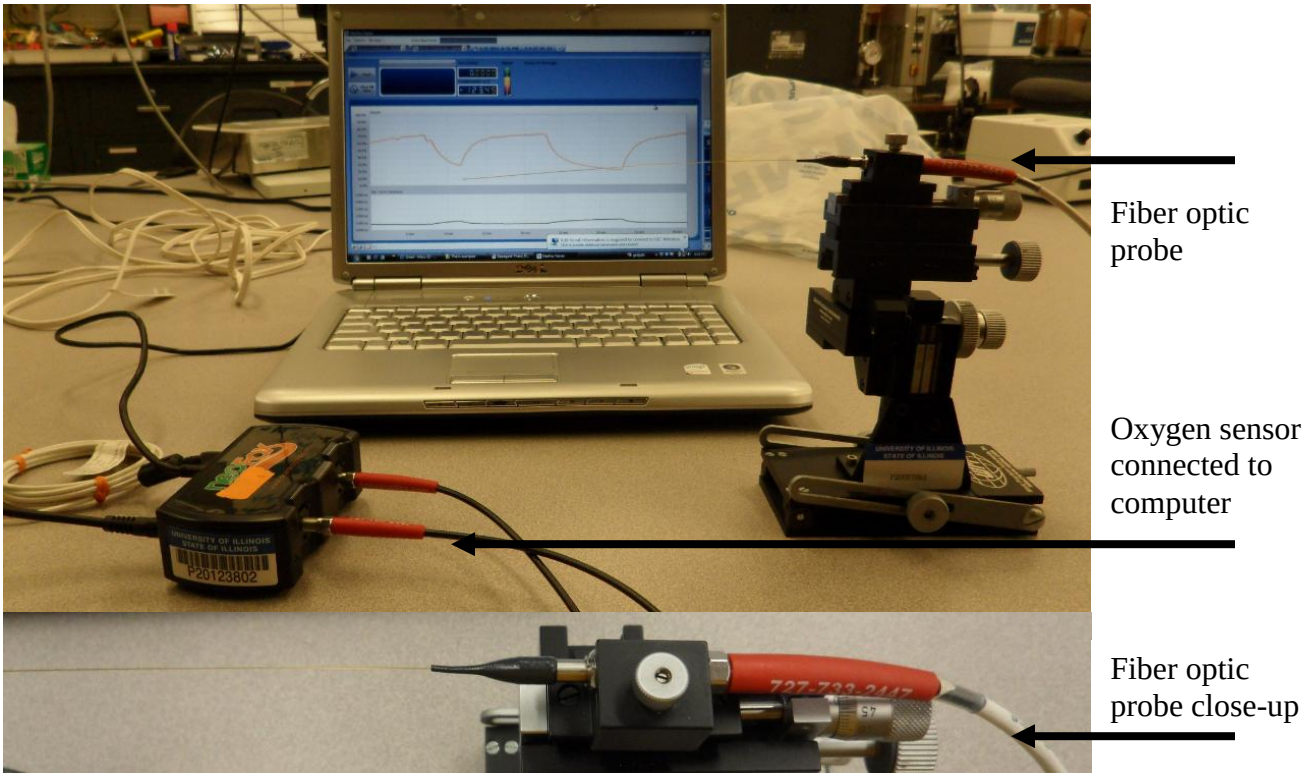

Fig. 2.5. Oxygen validating system. A hand-held oxygen sensor was used to measure the oxygen concentration produced by the device. Units used by the software are " % oxygen". The inset picture shows a magnified image of the fiber optic probe. The tip of the probe measures 15cm long and is connected to the sensor hardware.

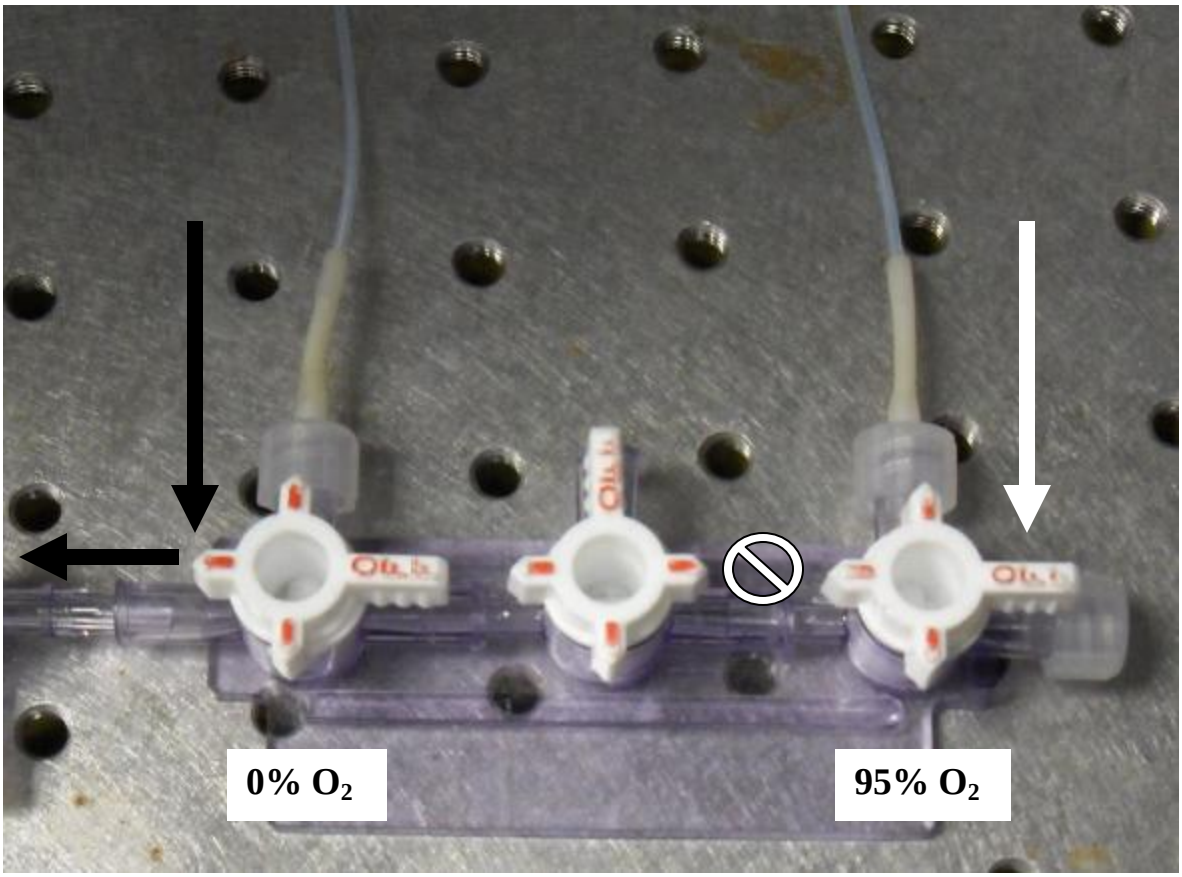

Fig. 2.6. Assembly used to deliver the different oxygen concentrations to the device. A 3-way stopcock was used to control what oxygen concentration was entering the device. The black arrow indicates the flow of direction. This set up allowed fast and efficient oxygen changes. In this particular set, 0% oxygen is flowing while the 95% oxygen flow is stopped.

2.2.1.3 –Temporal control over oxygenation

To begin the validation process of the microfluidic device, the temporal response of the device needed to be tested. Before using brain tissue in the validation studies, aCSF was used as the diffusion media. To start, the microfluidic device was filled with aCSF until it reached the top of the perfusion chamber.

Then, the oxygen probe was placed with its tip just above the surface of the PDMS membrane. In order to do this in a reproducible way, the probe was attached to an electronic micromanipulator (Siskiyou Inc.) capable of maneuvering the probe in the x, y, and z planes with a resolution of 0.1µm. As previously mentioned, the oxygen concentration was measured right above the surface: a height of 0µm. The experiment was also repeated at a height of 350µm, which represents the top of the slice.

Oxygen concentrations of 0% and 95% oxygen, both containing 5% CO_2 were introduced into the microchannel of the device and the oxygen concentration was measured using the oxygen probe.

2.2.1.4 –Spatial control over same channel

The oxygen concentration across one channel was measured using the oxygen probe in order to ensure homogeneity of the oxygen concentration. To do these measurements, the tip of the probe was placed at a height of 0µm using the electronic manipulator, and using the manipulators ability to move in the x and y plane, the tip was placed at predetermined spots in the channel and measurements were taken. The locations where the measurements were taken followed the path of the perfusing liquid.

The oxygen probe was placed at the first desired location, and 95% oxygen was introduced into the michochannel for 5 minutes, followed by 0% oxygen for 4 minutes, and then back to 95% oxygen for 21 minutes. The oxygen measurements were recorded and then the oxygen probe was moved to the next location and the cycle was again performed.

2.2.1.5 –Spatial control over multiple channels

In order to test the limits of the multi-channel design [Fig. 2.7], the oxygen concentrations across two channels were measured. Once again, using the oxygen probe attached to the electronic manipulator, the oxygen probe was placed at the 0µm height and then, using the channel wall as reference, the oxygen probe was placed at predetermined locations away from the channel wall.

Like in the previous experiment, 0% and 95% oxygen concentration gases were introduced into the microchannels and the oxygen concentration was measured at the predetermined locations. This experiment was performed in order to determine the minimum distance necessary to experience a completely different oxygen concentration. The oxygen concentrations were measured at a distance of 600, 500, 300, 200, 100, and 0µm away from the wall.

A)

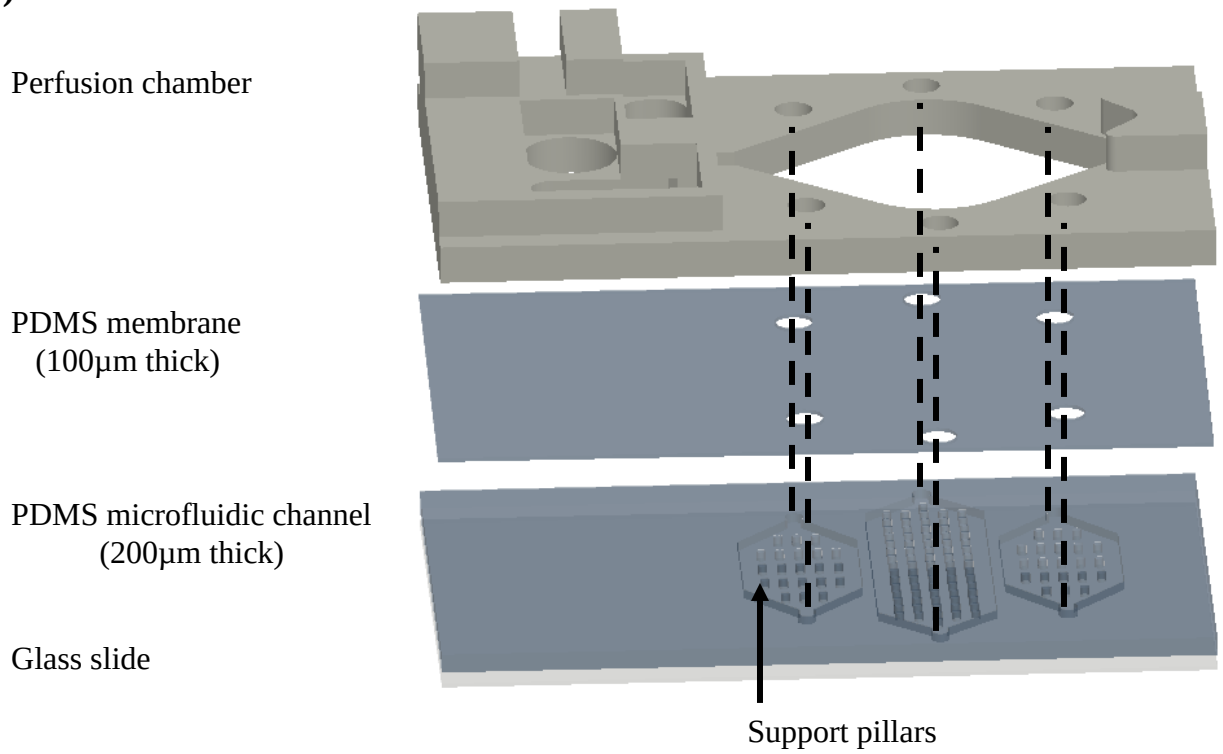

B)

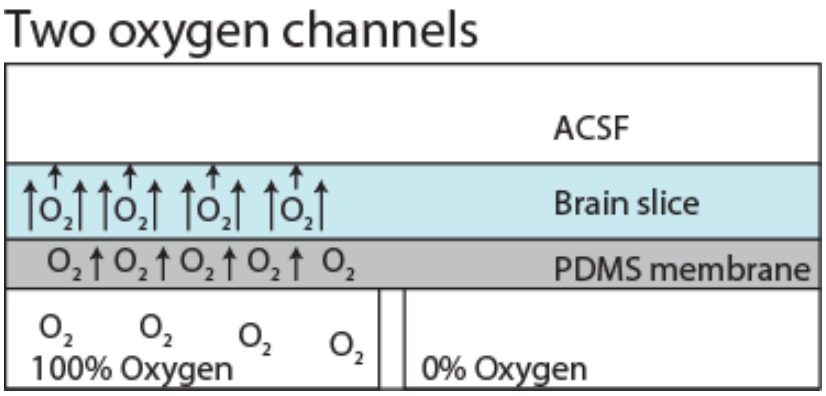

Fig. 2.7. Schematic of the microfluidic device. A) Exploded view of the multiple channel microfluidic device. As was the case for the single channel design, this device also consists of the perfusion chamber, the PDMS membrane, the PDMS microfluidic channel, and a glass slide. The dashed lines represent the inlets and outlets for all of the separate microchannels. B) Schematic describing how this version of the device works. As can be seen from the figure, the channel walls allow the device to create 2 different oxygen concentrations inside the tissue or the aCSF.

2.2.2 –Oxygen concentration in tissue as a result of the microfluidic device

For preliminary studies, the oxygen environment tested was aCSF; however, for the next part of the project, the oxygen concentration inside the brain slice was measured. Just like in the previous experiments, the oxygen probe was attached to an electronic manipulator. For the purposes of this study, the oxygen concentration at a height (starting from the bottom of the chamber) of 0, 100, 200, 300, and 350μm (top of the slice) were measured.

In order to perform the test, a brain slice was placed inside the finalized oxygen delivery device. Then, the chamber was filled with aCSF and the oxygen probe was placed right on top of the hippocampal CA1 area. Once the probe was in location, the oxygen concentration inside the brain slice was measured while different oxygen concentrations (0%, 95% O_2) were flowed inside the device.

2.2.3 –Oxygen concentration in aCSF as a result of the perfusion method

In a different set of experiments, the oxygen concentration of the aCSF was measured while it was being perfused. Rapid switching of oxygenated aCSF and deoxygenated aCSF provided the hypoxic insult previously provided by the microfluidic device. Just like in the previous experiments, the oxygen measurements were recorded using the hand-held oxygen probe attached to the electronic manipulator.

2.2.3.1 –Perfusion system

To start this part of the experiment, two glass flasks were filled with aCSF. Then, one of the flasks was oxygenated by bubbling with and 95% O_2/ 5% CO_2 gas while the other was depleted of oxygen by bubbling with 95% N_2/ 5% CO_2. The aCSF solutions were not used until

the solutions' oxygen concentrations were 91±2% O_2 and 3±2% O_2 as measured with the optical sensor.

As shown in figure 2.8, once the aCSF solutions were ready, the outlets of the flasks were attached to a 3-way stopcock that allowed rapid switching between liquid flows. The stopcock was then attached to medium diameter oxygen-impermeable tubing (Watson Marlow) that made its way into a peristaltic pump (403U/VM4, Watson Marlow) and then into the perfusion chamber where small diameter tubing (Watson Marlow) was used to provide the inlet flow. At the other end of the perfusion chamber, a metal adapter connected via medium diameter tubing to the peristaltic pump created a vacuum that provided an outlet for the perfusion flow. Ultimately, the perfusion flow was supplied at a rate of 2ml/min to the perfusion chamber.

2.2.3.3 –Temporal control over oxygenation

The temporal response of the oxygenation as a result of the perfusion method was tested in much the same way as it was for the microfluidic device. As was the case with the microfluidic device testing protocol, the aCSF solution's oxygen concentration was first measured. To start, the peristaltic pump, with the oxygenated flow on, was turned on and at a rate of 2ccm, the aCSF started to fill the perfusion chamber.

Then, the oxygen probe was placed with its tip at a distance of 350μm away from the bottom of the chamber, a location representing the top of the slices used in this project. After this, deoxygenated and oxygenated aCSF solutions were introduced to the perfusion chamber and the oxygen concentrations were measured with the oxygen probe. The oxygen concentration was measured at different locations in the perfusion chamber.

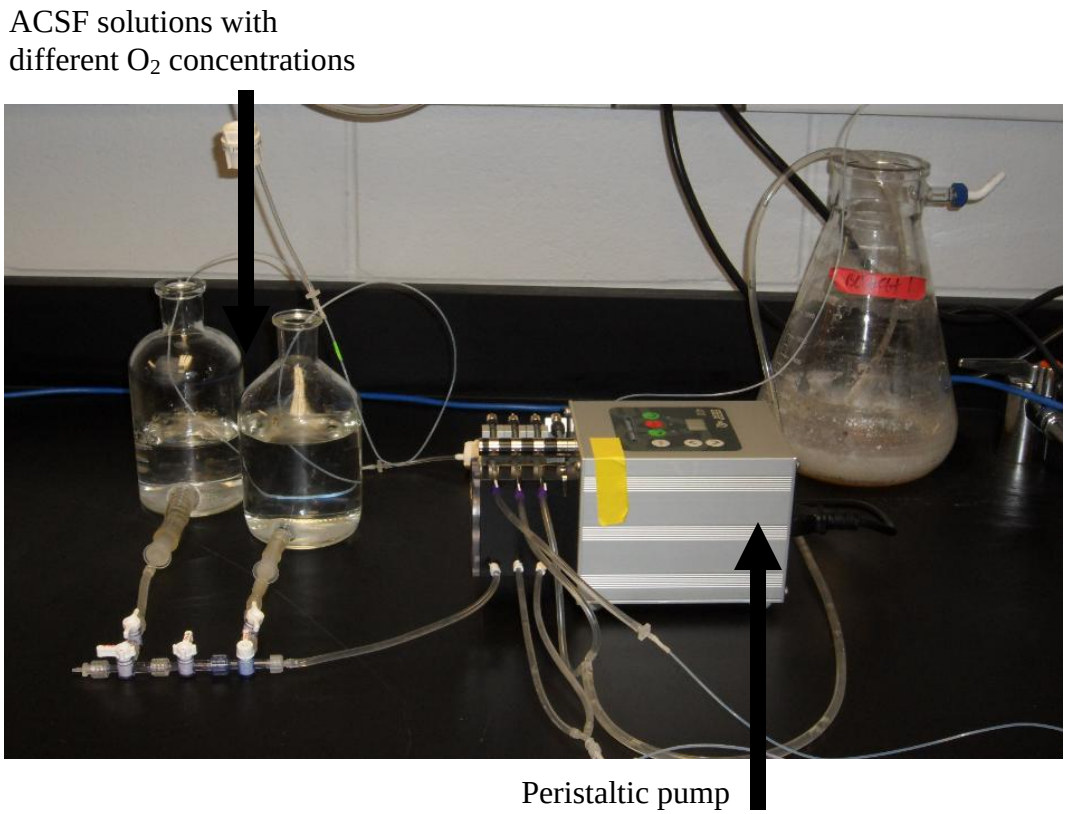

Fig. 2.8. Set up used for the perfusion method. A 3-way stopcock was used to control the liquid entering the perfusion chamber. The peristaltic pump controls the flow rate of the perfusing liquid. The aCSF solutions were constantly bubbled with different oxygen concentrations.

2.2.4 –Oxygen concentration in tissue as a result of the perfusion method

As was the case for the microfluidic device testing protocol, once the aCSF oxygen measurements were done, the next part of the project consisted on measuring the oxygen concentration inside the brain slice while cyclic oxygenated and deoxygenated flows were applied. In order to be consistent with previous experiments, the oxygen concentration at a height (starting from the bottom of the chamber) of 0, 100, 200, 300, and 350µm (top of the slice) were measured.

To start the experiment, the brain slice was placed inside the perfusion chamber and the perfusion was started beginning with the oxygenated aCSF. Then, the oxygen probe was placed right on top of the hippocampal CA1 area and the measurements began.

2.2.5 –Oxygen concentration in tissue as a result of the perfusion method and microfluidic device

Finally, in an effort to see the combined effect of the perfusion method and the microfluidic device, the oxygen concentration inside the brain slice was measured while both oxygenation methods were applied.

To perform this experiment, the brain slice was placed inside the microfluidic device and the perfusion was started beginning with the oxygenated aCSF. Then, the 95% oxygen gas was applied as previously described.

Once both oxygenation methods were being applied, the tip of the oxygen probe was placed on top of the CA1 area and oxygen measurements were taken at heights of 0, 100, 200, 300, and 350µm while cyclic oxygenation and deoxygenations were applied.

2.3 – Brain slice preparation

2.3.1 –Animals

The Animal Care and Use Committee at the University of Illinois Chicago approved all of the procedures outlined here. For this project, experiments were carried out on male and female wild type C57BL/6 mice (bred from stock obtained from Charles River Laboratories, Wilmington, MA). The experiments were conducted on mice at P17-22 (late postnatal).

2.3.2 –Slice preparation

The mice were deeply anesthetized using Aerrane (isoflurane, USP) and decapitated. Brains were rapidly removed from the skull and placed in chilled (3-7°C) cutting solution—high sucrose solution. Then, the cerebellum was separated and disposed, while the rest of the brain tissue was glued to an agar block with the cerebral cortex facing down. Next, while in chilled cutting solution, 350μm thick hippocampal slices were cut with a tissue slicer (Vibratome Series 1000 Classic) along the horizontal plane. The slices were then placed in a custom-made holding chamber containing cutting solution and incubated at 34°C for 35 minutes on a water bath (ISOTEMP 2025, Fisher Scientific). Then, the slices were transferred to another chamber containing artificial cerebral spinal fluid (aCSF) and incubated at the same temperature for 25 minutes. Following the incubation period, the brain slices were kept at room temperature. 95%O_2/ 5% CO_2 gas was continually bubbled into all solutions the brain slices were kept in. All experiments were performed at room temperature. Figure 2.9 shows the set up used for the dissection.

The cutting solution contained (in mM) 82.70 NaCl, 23.81 $NaHCO_3$, 2.41 KCl, 2.65 Na_2HPO_4, 10.50 $MgCl_2$, 0.38 $CaCl_2$, 23.70 Glucose and 71.19 Sucrose.

The aCSF solution used during slice incubation and experiments contained (in mM): 124.98 NaCl, 26.00 $NaHCO_3$, 2.50 KCl, 2.36 Na_2HPO_4, 4.27 $MgCl_2$, 2.00 $CaCl_2$, and 25 Glucose. The osmolarity of the solution was 300-310 mOsm, adjusted with sucrose. The solution had a pH of 7.4.

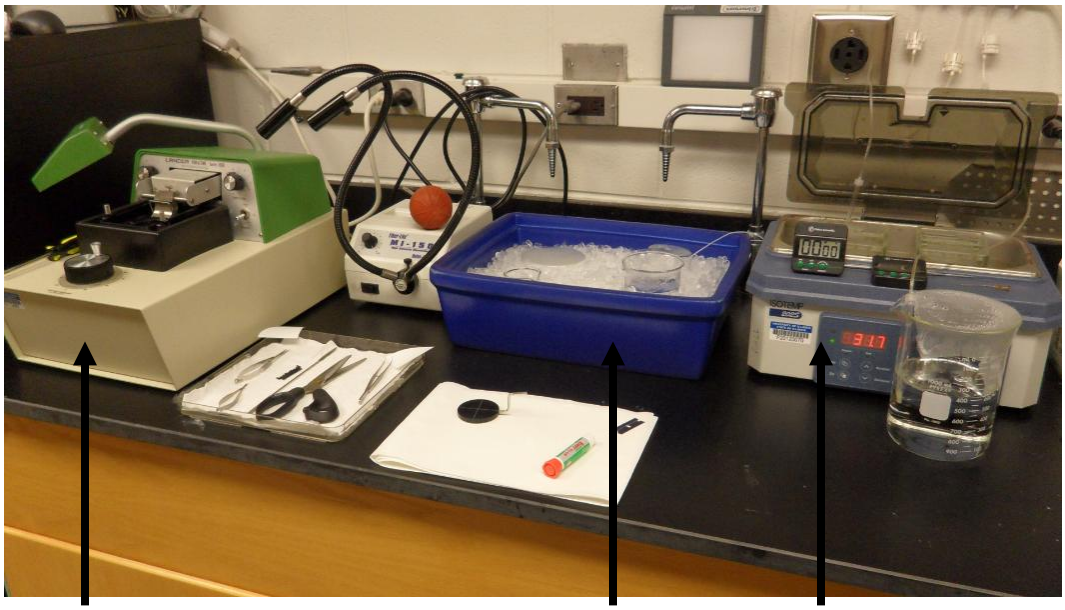

Fig. 2.9. Set up used during the dissection. The cutting solution was kept chilled during the dissection in order to optimize results. The stage of the tissue slicer was also kept cold during the dissection. The water bath was kept at 34°C.

2.4 – Validation of device via intracellular calcium response

2.4.1 –Fura-2/AM loading

In order to determine the intracellular calcium response of the brain slice, Fura-2/AM (acetoxymethyl ester) (Biotium) was used. A modified version of Yuste et al. (46) Fura-2 loading protocol was used to prepare the brain slices for imaging. After finishing the aCSF incubation period, the hippocampal brain slices were allowed to recover at room temperature for 10 minutes. During this time, the dye was prepared.

To prepare the dye, 5 µl of DMSO (Fisher Scientific) is added to a vial containing 2 µg of fura-2/AM; this solution is then mixed vigorously until a green color is observed. After this, 5 µl of Pluronic (Biotium) is also added to the vial and mixed until a uniform color is observed. The end result is a 5 µM membrane-permeable Fura-2/AM dye.

The protocol used for this project called for an incubation time of 60 minutes at room temperature. Due to this long incubation time, a customized microfluidic device was used to oxygenate the brain slices (21% O_2/ 5% CO_2). The microfluidic device, developed by Dr. Joe Lo, was originally developed for studies involving adherent mammalian cells [47] but was modified to serve our study. This device allows continuous oxygenation of the brain slices in a reservoir containing 1ml of Hepes solution.

Once the reservoir was ready and the dye was completed, the brain slices were placed in the reservoir and, using a 10µl pipette, the Fura-2/AM dye was puffed onto the brain slice focused on the hippocampal area. Then, the brain slices were incubated in a dark room for 60 minutes after which, the stained brain slices were transferred to the holding chamber containing oxygenated aCSF. The stained slices remained in this chamber until they were used for the experiment.

2.4.2 –Fluorescence imaging system

The images used to measure the calcium response were obtained using a fluorescent inverted microscope (Olympus IX71), a charged-couple device camera (QImaging Retiga-SRV) and using the image acquisition and analysis software MetaFluor Imaging System (Universal Imaging Corp) [Fig. 2.10].

In order to obtain the required images, a stained brain slice was transferred to the microfluidic device and submerged in aCSF. Then, a motorized stage (Prior ProScan II) was used to center the visual field on cell bodies from the hippocampus, CA1 area unless otherwise noted. The samples were alternatively excited with 340- and 380-nm wavelengths and detection of fluorescence emission at 510nm; the pictures were acquired using the 20X objective. All images were acquired at room temperature unless otherwise noted. Image intensities were exported using Metamorph for later analysis using Microsoft Excel.

A modified version of Yuste et al. (46) Fura-2 image analysis was used for our analysis. The Fura signal has a Y-axis labeled "percent change". These units were used in order to quantify the change in the signal intensity during the hypoxic period compared to the 5-minute baseline period. The following formula was used to obtain this set of units:

$$Percent\ Change = \left(\frac{\left(Current\ Point - Baseline \right)}{Baseline} \right) * 100 \qquad (2.4)$$

where the baseline value represents the average value of the initial 5 minute oxygenation period, and the current point represents each data number obtained during the experiment.

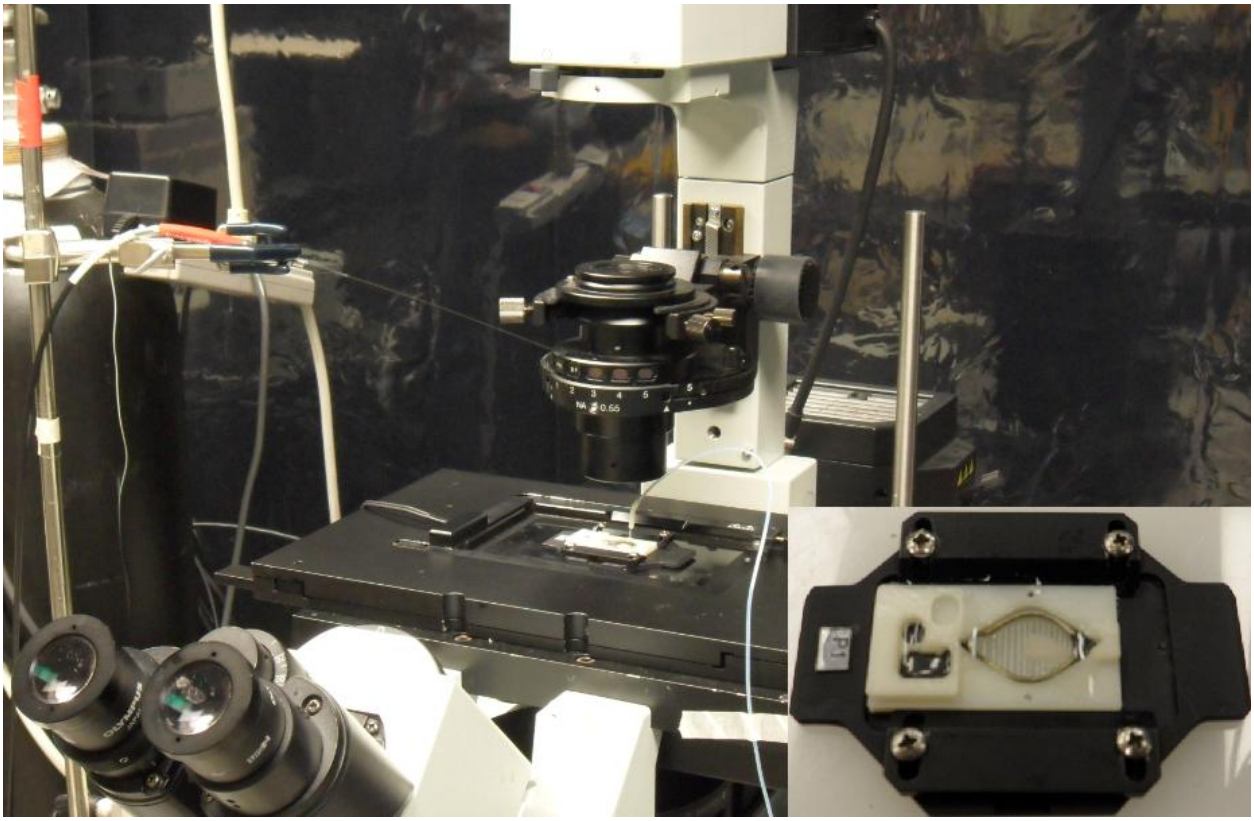

Fig. 2.10. Set up used for Fura validation experiments. A fluorescent-equipped microscope was used to acquire images of the ratiometric calcium indicator using Metamorph image acquisition software. The obtained images were analyzed using Excel. Experiments using the perfusion method or the microfluidic device were done using this set up. The inset picture shows a magnified view of the microfluidic device inside the stage.

2.4.3 –Exposure of brain slice to hypoxic insult using perfusion

As was the case for the oxygen concentration validation protocol, the oxygenated perfusion was applied at a rate of 2 ml/min using a peristaltic pump.

Once the perfusion had started and the CA1 area was in the visual field, an average of 8-13 cell bodies were selected using the "region of interest" function from the MetaFluor software. Then, a series of images was recorded every 20 seconds for 30 minutes beginning 5 minutes before switching to the hypoxic solution.

5 minutes of oxygenated aCSF were followed by 4 minutes of deoxygenated aCSF and the rest of the time was switched back to the oxygenated solution. The aCSF levels were carefully monitored in order to avoid overflow, as leaking solution could damage the microscope beneath the perfusion chamber.

2.4.4 –Exposure of brain slice to hypoxic insult using device

In order to be consistent in all experiments, the same time frames of oxygenation and deoxygenation were applied using the microfluidic device. Once the brain slice was in place and the adequate cell bodies were selected, images 20 seconds apart were recorded for 30 minutes.

Using a flow rate of 38ccm, 95% O_2 gas was inserted into the microfluidic device followed by 0% O_2 gas. For this experiment, the microfluidic device with the single channel design was used. The aim of this initial test was to validate the microfluidic device and compare it to the perfusion method.

2.4.5 –Spatial control over multiple channels

Once the microfluidic device with the single channel design was tested, the design that had multiple channels had to be tested as well. As was previously mentioned, the microfluidic device allows multiple oxygen concentrations to affect different parts of the brain slice. For the following experiment, the hippocampal CA1 and dentate gyrus area were imaged.

2.4.5.1 –DG and CA1

In order to simulate a stroke, a brain slice was placed in the microfluidic device and manipulated in such a way that the dentate gyrus was on top of one of the channels, while the CA1 area was on top of a separate channel. After this, the imaging procedure took place in two steps. First, the visual field was centered on cell bodies from the hippocampal CA1 area. Then, the CA1 area was exposed to different oxygen concentrations (0%, 95% O_2), while the rest of the slice was experiencing a constant oxygen environment (95% O_2). The images were taken and analyzed.

During the second part of the experiment, the visual field was centered on cell bodies from the dentate gyrus area from the hippocampus. In much the same way as before, the dentate gyrus was exposed to different oxygen concentrations (0%, 95% O_2), while the rest of the slice was experiencing a constant oxygen environment (95% O_2). The images were taken and analyzed.

The experiment was performed this way for two reasons. First, the MetaFluor imaging system cannot take images from different areas of the slice during the course of a single experiment. Second, even if the system could take images from different areas, it would be

unwise to do so as even a small movement of the cell bodies could add noise to the response signal.

Finally, the dentate gyrus and the CA1 area imaged while they were experiencing a constant oxygen environment.

2.4.5.2 –Distances from the wall

In order to test the limits of the microfluidic device, the brain slice was imaged at predetermined locations and the necessary distance to obtain a favorable Fura response was determined. Just as was the case for the oxygen concentration validation protocol, images were taken at a distance of 600, 500, 300, 200, 100, and 0µm away from the wall. Like in the previous experiments, 0% and 95% oxygen concentration gases were introduced into the microchannels and the Fura response was measured at the predetermined locations.

2.4.5 –Increased spatial resolution using a cover slip

The spatial resolution of the device was increased in order to deliver a point source of hypoxia; this was done in an attempt to better simulate a stroke *in vitro*. The increase in resolution was accomplished thanks to a standard round cover slip with a 1mm hole drilled into it. Once the whole was made, it was placed on the microfluidic device in the middle of the bath area. After this, the brain slice was placed on top of the coverslip making sure to place the CA1 area of the hippocampus right on top of the drilled hole. Once everything was set up, 95% O_2 was fed into the microchannel followed by 0% O_2 just like in previous experiments, Fura-2 images were taken and analyzed.

CHAPTER III: Results

3.1 - Oxygen concentration validation measurements

The oxygen concentration experienced by the brain slice was measured using a hand-held oxygen sensor. The results demonstrate that the microfluidic device can effectively establish an environment of different oxygen concentrations in short timescales and with high spatial resolution, something that is not possible with the perfusion method.

3.1.1 –Oxygen concentration in aCSF as a result of the microfluidic device

A hand-held fluorescent-based optical oxygen sensor (Neofox, Ocean Optics) was used to quantify the oxygen concentration experienced by the brain tissue. The cyclic 0-95% oxygen experiments demonstrate that the device can rapidly change the oxygen concentration when the aCSF is used as the diffusing media and as shown in figure 3.1, there is not significant change in the oxygen concentration between the bottom of the device (0µm) or the top of the liquid (350µm). When the oxygen concentration is measured at a height of 0µm, the device can equilibrate to 95% in about 1 minute and can reach a value of less than 9% oxygen in less than a minute and reach a minimum value of 5% after 4 minutes.

In order to ensure homogeneity of the oxygen concentration, oxygen measurements were also taken across the width of the channel at predetermined locations. Oxygen concentrations of 0% and 95% oxygen were introduced into the microchannel of the device and the oxygen measurements were recorded as shown in figure 3.2. The seven different locations were tested without any significant change from one another signifying a homogeneous oxygen environment across the channel.

The oxygen concentration across two channels was measured in order to prove that two different oxygen concentrations could be established within the microfluidic device. Taking the channel wall as a reference, five locations away from the wall were used to take measurements. Figure 3.3 shows how two distinct oxygen concentrations can be produced with 100μm being the necessary distance for the oxygen concentrations to be completely different.

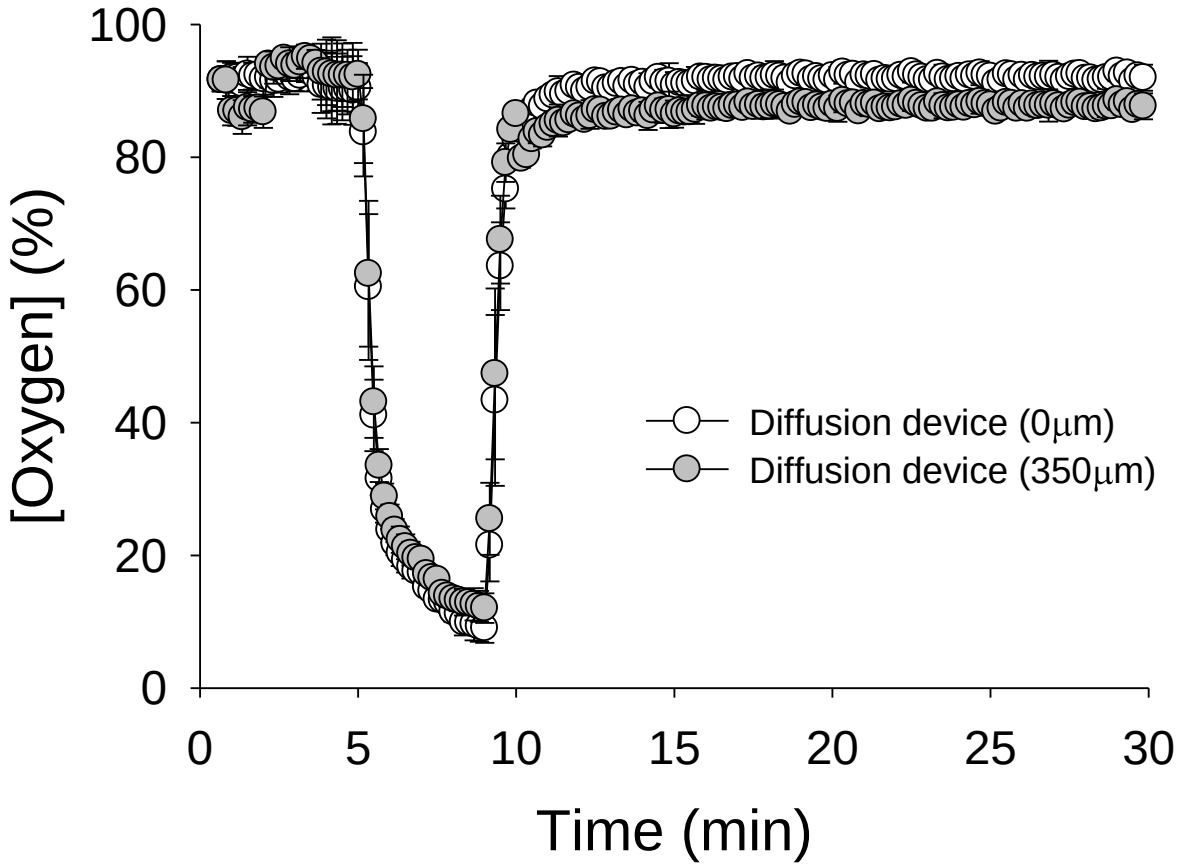

Fig. 3.1. Oxygen measurements in aCSF for two different heights. Using a hand-held oxygen probe, the oxygen concentration dissolved in aCSF was measured. The gas fed into the device was cycled between 95% and 0% oxygen. By doing this, the device mimics a hypoxic insult to the tissue. As can be seen, the device can equilibrate in a short amount of time and can obtain a uniform oxygen environment with no significant difference between the bottom or the top of the device.

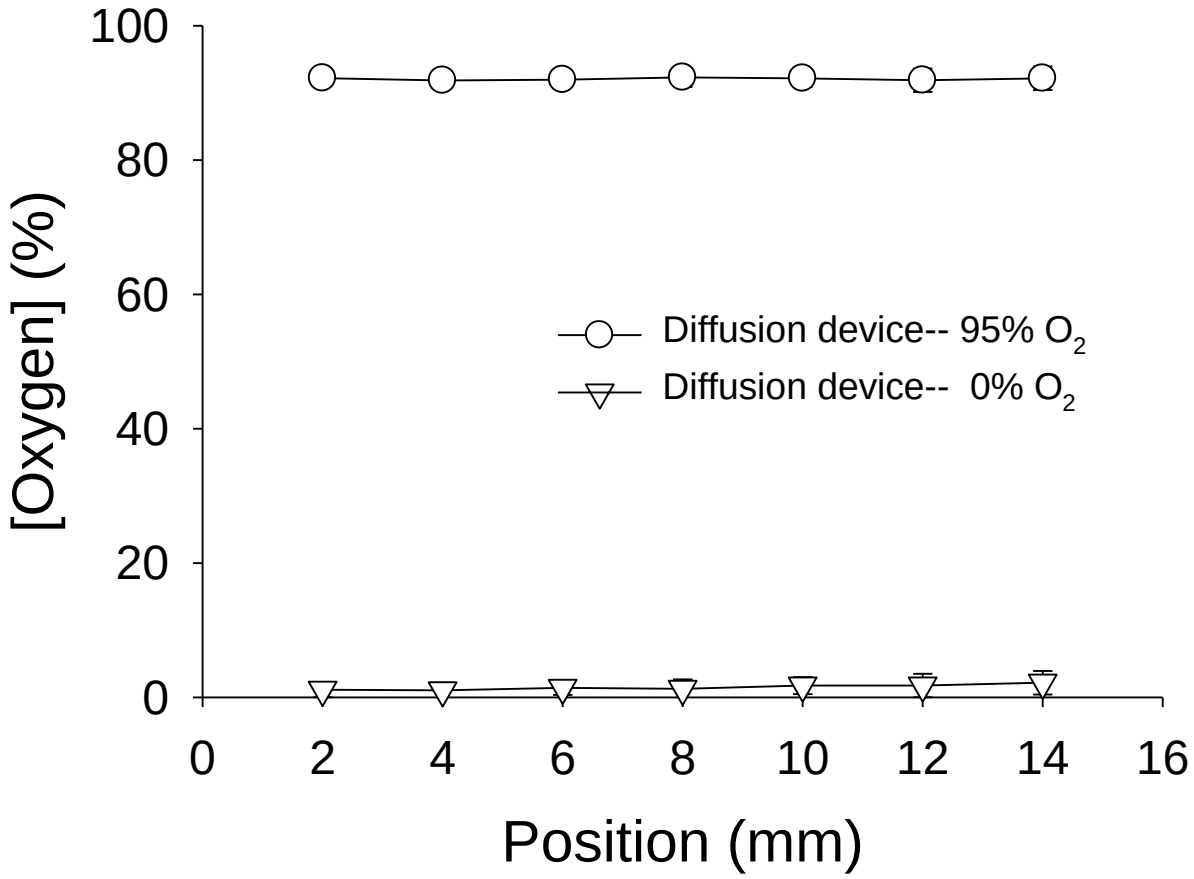

Fig. 3.2. Validation of the microchannel. Using a hand-held oxygen probe, linescans were taken across the microchannel to make sure that the device produces a homogeneous oxygen environment. The graph shows the values obtained after 0% and 95% oxygen were introduced into the microchannels.

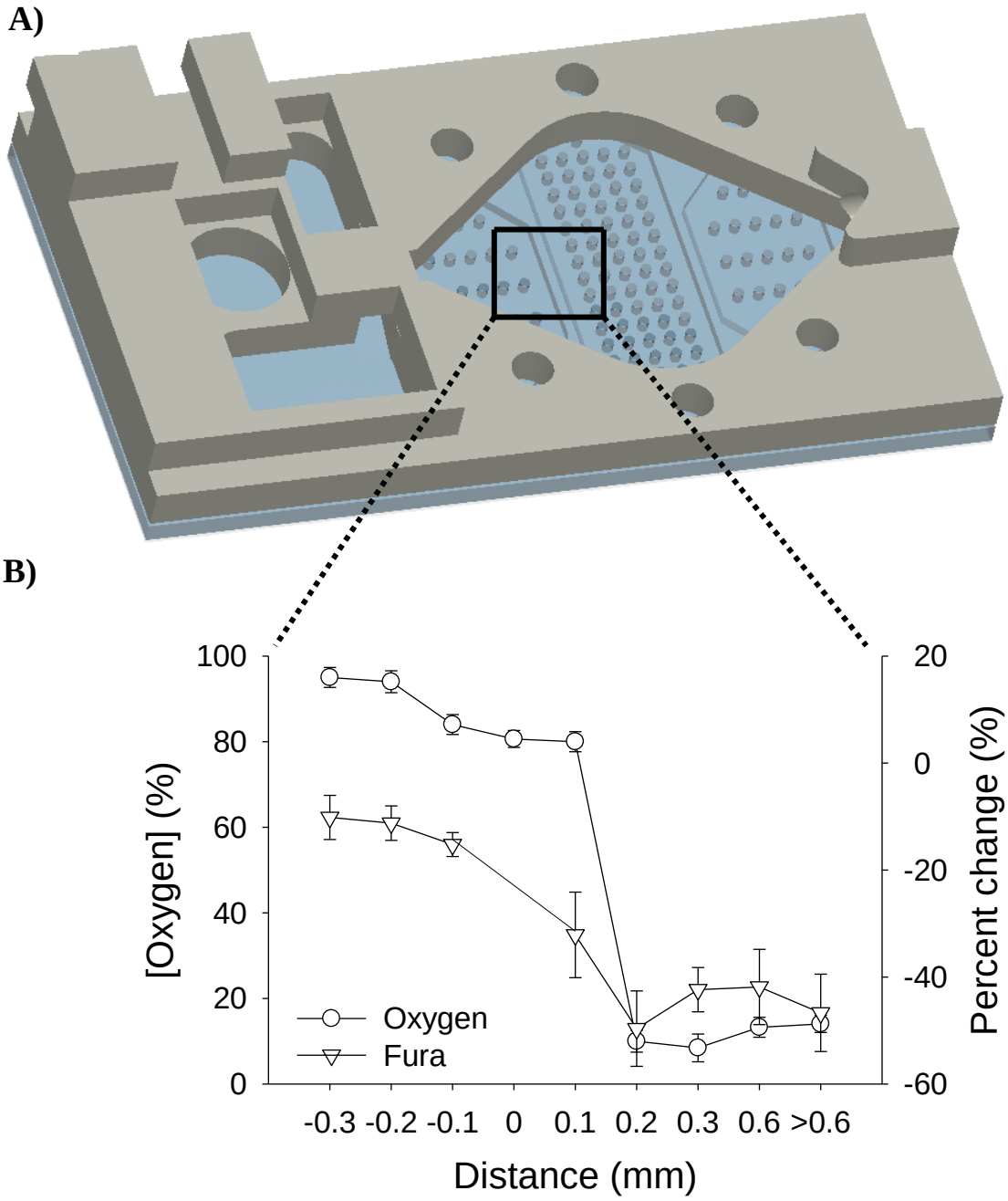

Fig. 3.3 Schematic and validation of a microfluidic device capable of spatio-temporal oxygen control. A) Image showing the completed microfluidic device used to oxygenate different regions of the brain. This device consists of 4 independent parts: the perfusion chamber, the PDMS membrane, the PDMS microfluidic channels, and a simple glass slide. The square shows the location where the measurements for B were taken. B) In order to test the limits of the device, the oxygen and Fura measurements were taken at certain distances away from the microfluidic channel walls. One channel is flowing 95% oxygen while the other one is flowing 0% oxygen. As shown, the oxygen measurements take a steep change from one microfluidic channel to the adjacent one. The Fura signal shows a similar change from one channel to the other.

3.1.2 –Oxygen concentration in tissue as a result of the microfluidic device

After obtaining favorable results with the aCSF oxygen experiments, the next part of the project involved determining the oxygen concentration within the tissue itself. Using the electronic manipulator, the oxygen concentration at heights of 0, 100, 200, 300, and 350µm were measured. As shown in figure 3.4, the minimum and maximum values were recorded. The minimum values were measured 4 minutes after the 0% oxygen started flowing inside the device while the maximum values were measured after 5 minutes of the switch to the 95% oxygen gas and the concentration had equilibrated. From the graph, a distinct gradient is evident when the 95% oxygen is flowing, however, the device does a remarkable job at keeping a constant oxygen environment throughout the entire slice while the 0% oxygen is flowing.

3.1.3 –Oxygen concentration in aCSF as a result of the perfusion method

Using a standard perfusion set up, the oxygen concentration within the aCSF as a direct result of the perfusion method was quantified. The temporal response of the perfusion method was tested in a similar way as the microfluidic device. Using the oxygen sensor probe at a height of 350µm, the oxygen concentration was measured while the perfusing liquid was cycled from oxygenated aCSF to deoxygenated aCSF. Also, the oxygen concentration across the perfusing chamber was measured and the results are shown in figure 3.5. As seen in this figure, the perfusing liquid does in fact provide a homogeneous oxygen environment throughout the perfusing area.

A)

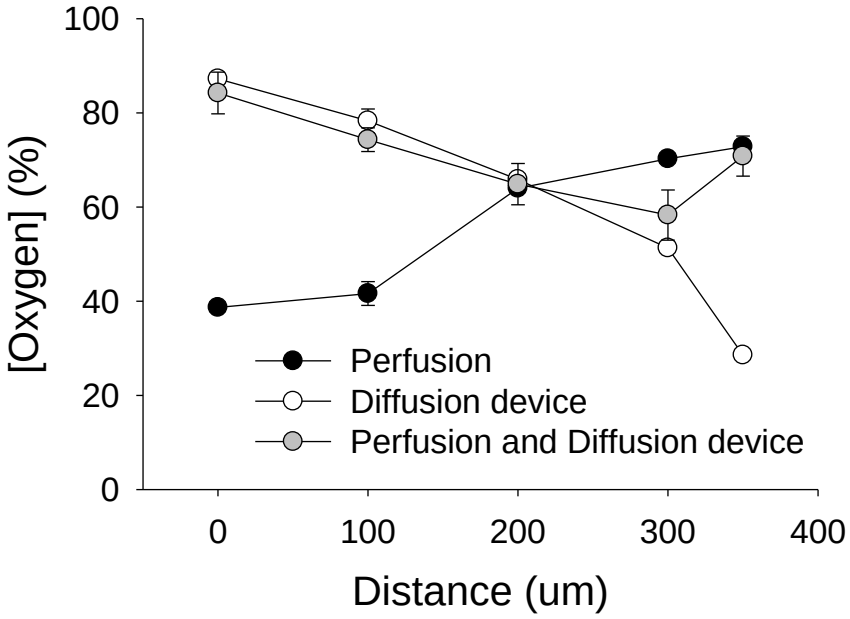

B)

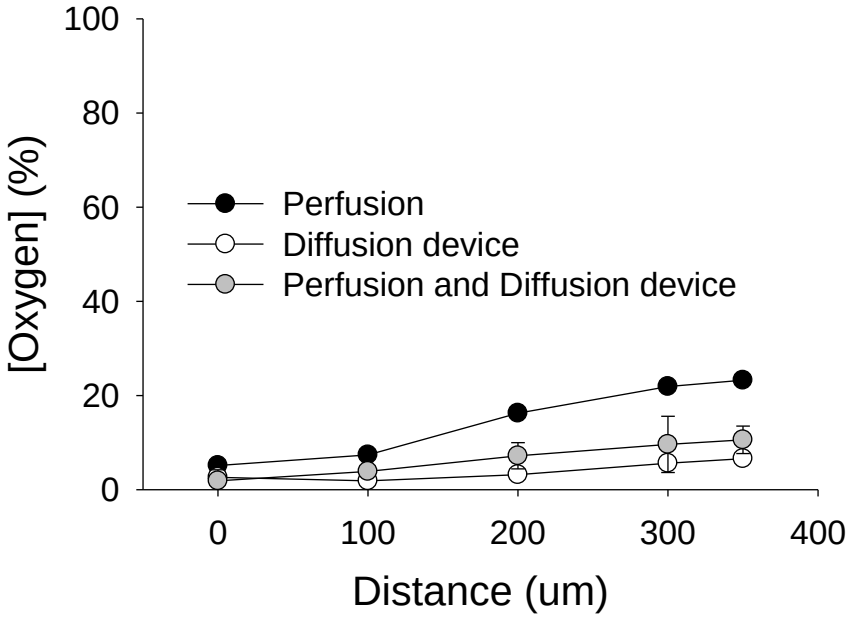

Fig. 3.4. Oxygen concentration inside the brain slice. A) Using a hand-held oxygen probe combined with an electronic manipulator, the oxygen concentration reaching the brain slice at specific locations was measured. Oxygen concentration at a depth of 0, 100, 200, 300, and 350μm were measured. Perfusion and device measurements are recorded. The graph shows the maximum concentrations obtained at different distances. B) The graph shows the minimum levels obtained from the different methods.

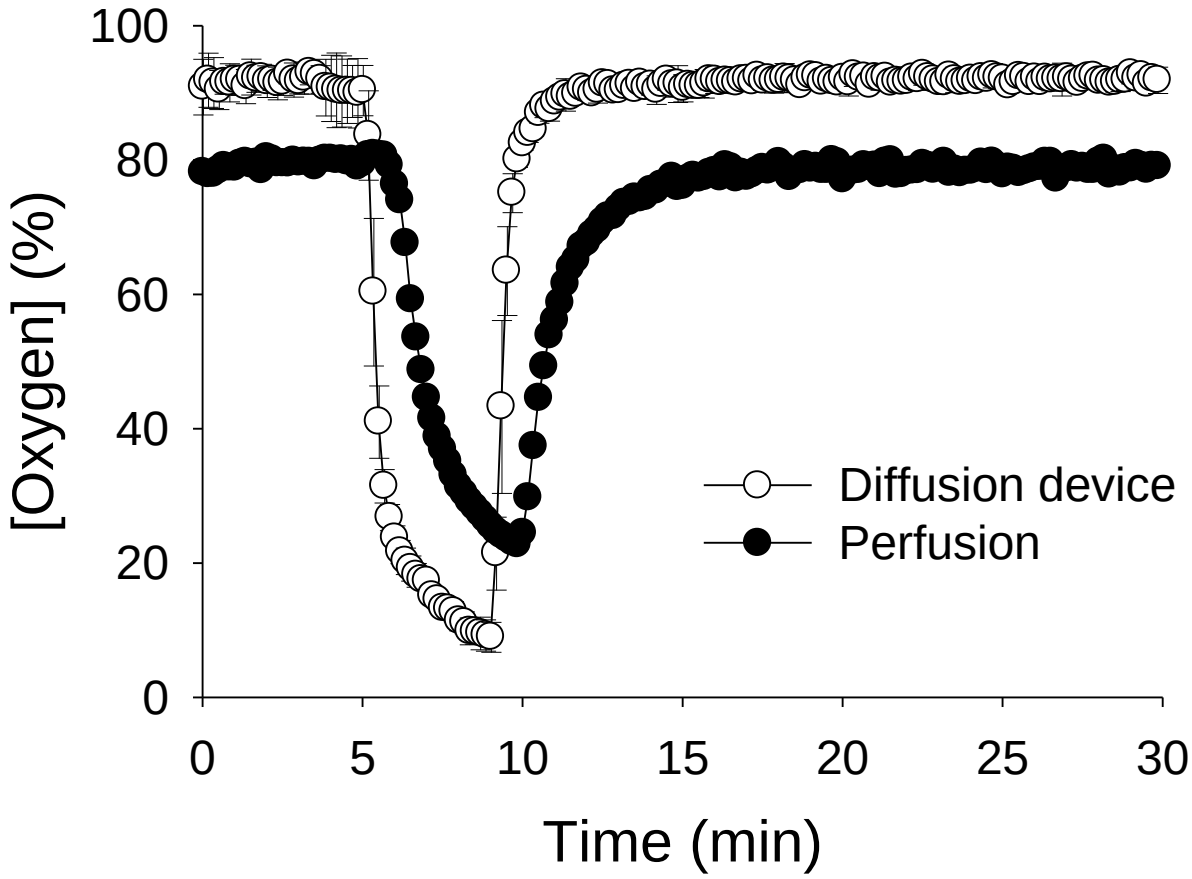

Fig. 3.5. Oxygen measurements in aCSF for two different methods. Using a hand-held oxygen probe, the oxygen concentration (dissolved in aCSF) reaching the brain slice was measured. The graph shows the results for the perfusion method as well as the microfluidic device method. The device obtains a more controlled as well as a bigger change in oxygen concentration.

3.1.4 –Oxygen concentration in tissue as a result of the perfusion method

Once again, the oxygen concentration inside the brain slice was measured using the oxygen probe at heights of 0, 100, 200, 300, and 350μm. In figure 3.4, the minimum value was measured at the end of the hypoxic period, while the maximum value was measured five minutes after the hypoxic period had ended and the oxygen concentration had equilibrated.

3.1.5 –Oxygen concentration in tissue as a result of the perfusion method and microfluidic device

The combined effects of the perfusion method and the microfluidic device on the oxygen concentration inside the tissue are shown in figure 3.4. This experiment was done in order to see if by combining both methods a constant oxygen environment throughout the entire slice could be achieved. Once again, the oxygen concentrations were measured at predetermined locations inside the tissue while cyclic oxygenation and deoxygenations were applied. From figure 3.4, it can be seen how the oxygen concentration within the tissue is relatively constant from one end of the slice to the other end.

3.2 – Validation of device via intracellular calcium response

Using a fluorescent microscope and the Fura-2 dye, the brain slice's response to hypoxia was measured. The results demonstrate that the microfluidic device can effectively deliver a hypoxic insult to the neuronal cells in a rapid and controlled manner and more importantly, the microfluidic device is able to selectively deoxygenate specific areas of the brain slice while leaving the rest of the brain slice intact, something that is not possible with any current methods.

3.2.1 –Exposure of brain slice to hypoxic insult using perfusion

Using the perfusion method to deliver a hypoxic insult is one of the basic techniques in neuroscience. As shown in figure 3.6.A, this method can clearly deliver the necessary deoxygenation to obtain a response from the neuronal cells, however, the perfusion's Fura response extended for a period close to ten minutes, long after the deoxygenation should have stopped. Moreover, the Fura response was in the range of 30% with respect to the baseline, which agrees to the incomplete deoxygenation provided by the perfusion.

3.2.2 –Exposure of brain slice to hypoxic insult using device

Using the microfluidic device and a fluorescent microscope, the calcium response in the neurons from the CA1 area of the hippocampus was imaged in order to determine the relationship between neuronal function and hypoxia. Figure 3.6.B shows the cyclic oxygenation and deoxygenation experiments which demonstrate that the microfluidic device is able to deliver a hypoxic stimulus and a clear response, in the form of a dip in the Fura's intensity signal, is obtained. The device's Fura response is clearly constrained to the four minutes in which the deoxygenation occurred and has a magnitude of close to 50% change with respect to the baseline, which agrees with the deeper hypoxia provided via diffusion in the new device.

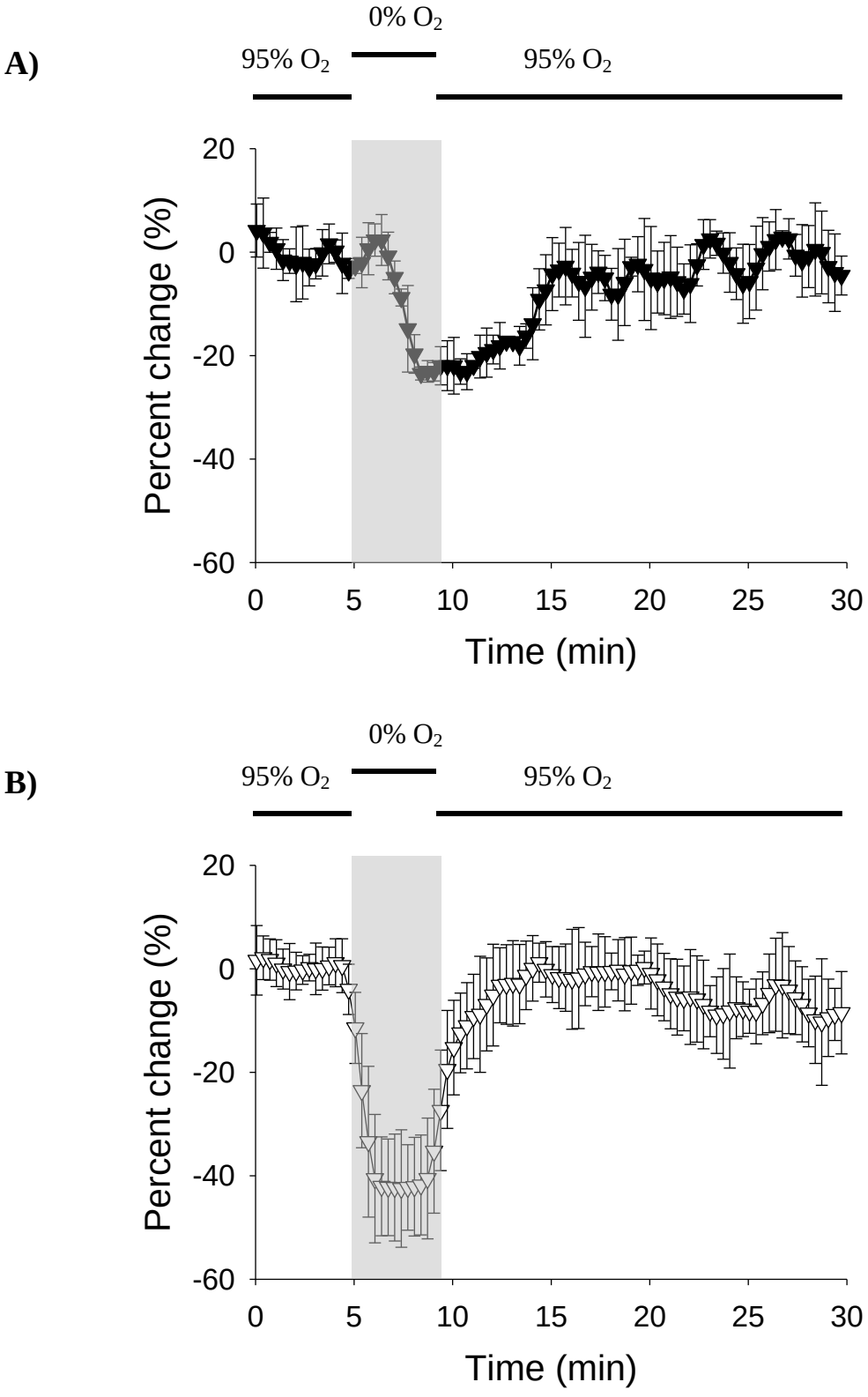

Fig. 3.6. Fura readings for the two methods studied. A) Graph showing the Fura signal obtained by the perfusion method. Decreases in signal intensity signify and increase in intracellular calcium. The hypoxic period is represented by the blue rectangle. B) Graph showing the Fura signal obtained by the diffusion device.

2.4.5 –Spatial control over multiple channels

One of the highlights of the microfluidic device is its ability to deliver multiple oxygen concentrations to different areas of the brain slice. In figure 3.7, two different Fura responses are shown corresponding to the Fura response of the dentate gyrus and the CA1 area. As shown in this graph, while the CA1 area was stimulated with a hypoxic insult, the dentate gyrus was allowed to keep a constant oxygen environment. These differences in oxygen concentration give rise to the change in Fura response from these two areas. While the dentate gyrus shows no sign of change throughout the entire experiment, the CA1 area shows the distinctive dip corresponding to the hypoxic insult.

In figure 3.3, an experiment aiming to test the limits of the microfluidic device is shown. During this experiment, the device using the multiple channel design was used to figure out what was the necessary distance away from the channel wall necessary to obtain a different Fura response. Images were taken at a distance of 600, 500, 300, 200, 100, and 0µm away from the wall. From the graph, it is evident that at a distance of 200µm away from the wall, the neuronal cells are able to produce a favorable Fura response.

2.4.6 –Increased spatial resolution using a cover slip

As previously stated, with this device, different areas of the brain slice can be stimulated with different oxygen stimuli; however, in certain cases, a more refined stimulus may be necessary. With this in mind, a coverslip with a 1mm diameter hole was used in order to isolate the CA1 area. Figure 3.8 shows how the exposed area responds to the hypoxic insult in much the same way as the previous experiments.

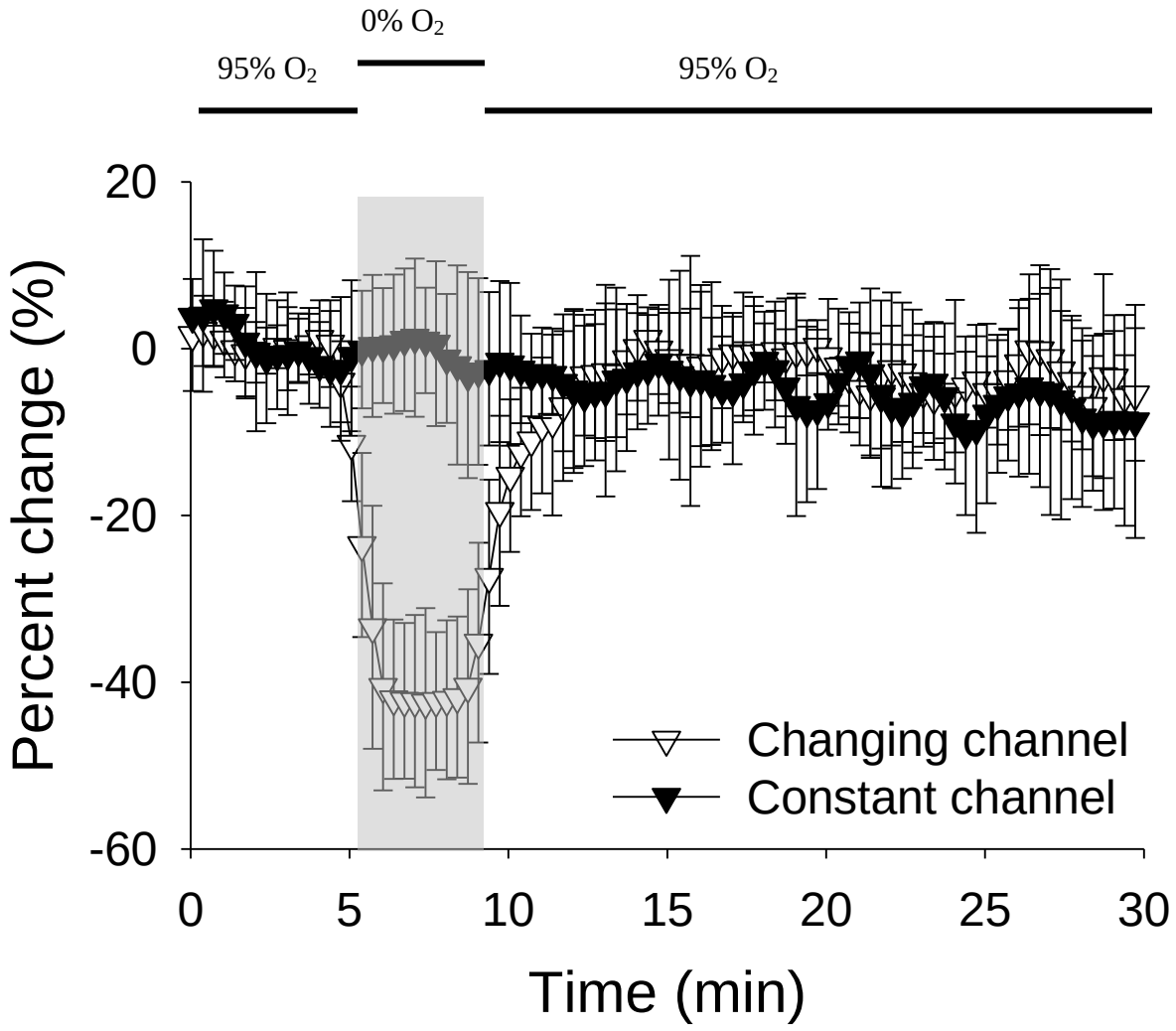

Fig. 3.7) Fura readings from two different hippocampal regions. As indicated from figure 3.3, the microfluidic device is able to maintain 2 different oxygen concentrations in different parts of the same brain slice using microchannels. Here, the brain slice was positioned in such a way as to have the CA1 in one michochannel and the dentate gyrus in a second microchannel. The CA1 area was exposed to a hypoxic insult while the dentate gyrus was kept to a constant oxygen environment. As expected, the CA1 area experienced an increase in intracellular calcium while the dentate gyrus did not suffer a change in calcium concentration.

A)

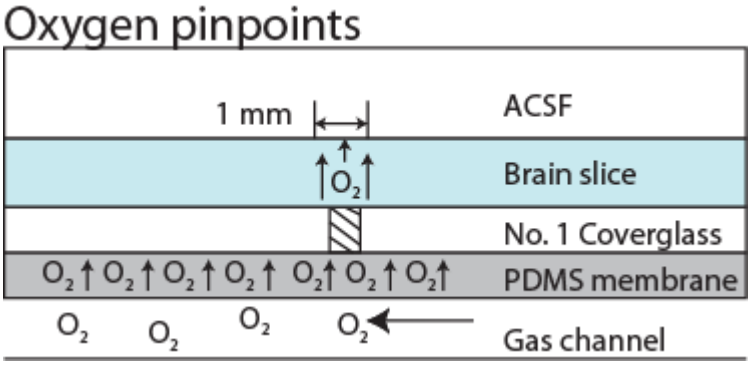

B)

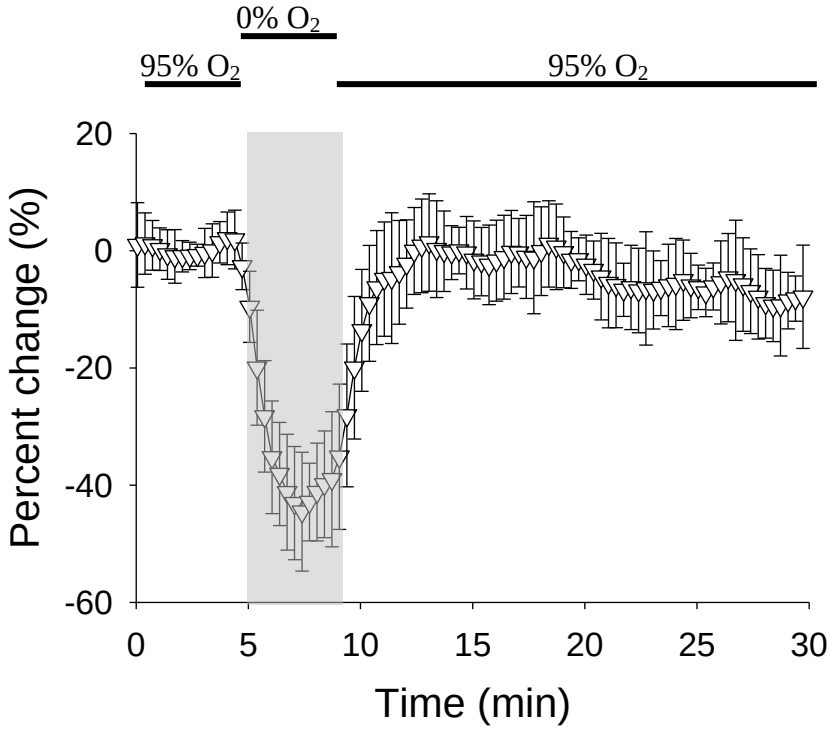

Fig. 3.8. Manipulation of size and shape of stimulated area. A) Diagram showing how a glass coverslip can be used to manipulate the size of the stimulated area in the brain slice. The hole in the coverslip allows the oxygen to flow into the tissue and can be made as big or small as desired. B) Fura measurements obtained from the stimulated area of the brain slice. The CA1 area was solely exposed to the hypoxic insult and as expected, the hole in the coverslip was big enough to produce a change in intracellular calcium

CHAPTER IV: Discussion

4.1 –Advantages of the microfludic device

4.1.1 –Temporal oxygen precision

Until now, localized deoxygenation of a brain slice was not possible in a way suited for stroke research. A convenient feature of the device is its noninvasive nature; by diffusing throughout the PDMS membrane, the oxygen gas does not disturb the slice. This is a convenient way to oxygenate the slice while avoiding problems associated with gas pressure destroying the brain tissue (9). Using our add-on microfluidic device, we can adjust the oxygen environment within a matter of minutes.

As seen in figures 3.1 and 3.2, the microfluidic device is able to create a constant environment all across the channel as well as a constant oxygen environment in the Z-direction as long as the diffusion media is aCSF. As was proved in future experiments, this is not the case if the diffusion media is a solid tissue.

The microfluidic add-on and the perfusion method are both capable of delivering a supply of oxygen to the brain slice. The device allowed complete temporal control over the hypoxic insult and is able to reach greater differences in oxygen concentration when compared to the perfusion method. The device is capable of creating a hypoxic environment in less than four minutes and is able to revert back to its initial settings in the same amount of time compared to perfusion, which requires over eight minutes to equilibrate. It is also capable of achieving a level of hypoxia of 9% as compared to the perfusion method, which was only able to achieve 22%.

In order to show the usefulness of this device to neuroscience research, we imaged the calcium response in the neurons from the CA1 during a hypoxic insult. Slices were exposed to a

hypoxic insult mediated either by the microfluidic device or by the perfusion method. Even though both methods were able to deliver the hypoxic stimuli and a response was obtained for each, there is a clear difference between the two signals. The device's Fura response is clearly constrained to the four minutes in which the deoxygenation occurred, while the perfusion's Fura response extended for a period close to ten minutes, long after the deoxygenation should have stopped. Moreover, the device's Fura response had twice the magnitude as the perfusion's response, which agrees with the deeper hypoxia provided via diffusion in the new device.

4.1.2 –Ability to obtain a constant oxygen environment

The oxygen within the tissue will ultimately guide the neuron's response. Common methods use only perfusion to oxygenate a brain slice (32), however, the end result is lower oxygen condition in the middle of the slice when compared to the outer edges of the slice (3, 35, 48). Some newer methods modify the perfusion chamber in such a way as to elevate the slice in an attempt to have fluid flowing above and below the slice (34), however, even with this modification, an oxygen gradient within the slice is still created. By measuring the oxygen concentrations inside the brain slice at predetermined positions [Fig. 3.4], we demonstrated that our device created a noticeable gradient as the diffusion distance increased. This gradient moved in the opposite direction as the gradient produced by the perfusion method. In an effort to create a constant oxygen environment throughout the brain slice, we combined the device with the perfusion method and found that a relatively uniform oxygen environment is created in the brain slice with the device dominating on the lower part of the slice and the perfusion dictating oxygen concentration on the top of the slice.

While the ability to fully oxygenate the slice is a remarkable achievement, and one that has inspired several microfluidic devices (34, 49, 50), it is not a necessity for most brain slice experiments, especially ones aiming at discovering the effect of oxygen on neuronal tissue. From our results, we demonstrated that even though the device does not create a uniform high oxygen environment, it is capable of producing a uniform hypoxic environment throughout the entire slice with only an 8% difference from the bottom to the top of the slice, while perfusion creates a gradient of over 20% from top to bottom. These data suggest that the device is both capable and efficient at producing hypoxic insults on the brain tissue in a well-controlled manner superior to current methods.

Even if measurements from the top of the slice are needed, as is the case when using electrophysiology tools, we are confident that the microfluidic device alone is capable of delivering a hypoxic insult to the cells all throughout the brain slice. Based on the data obtained from the top of the slice, we were able to implement a significant hypoxic insult to the tissue, an oxygen difference of more than twenty percent.

4.1.3 –Spatial oxygen precision

In order to provide not only temporal control, but also achieve spatial control, a second microfluidic device was created. This second device works under the same principle as the original device except that in this case, several independent microchannels can supply different regions of the slice with different oxygen concentrations. For this project, the microfluidic channel was customized to allow the CA1 and the dentate gyrus to experience different oxygen environments.

As in the previous device, we validated the functionality of the device by measuring the oxygen delivery and by recording the Fura response when the tissue is stimulated by oxygen. Since we wanted to determine the limits of the device, the oxygen and Fura measurements were taken at certain distances away from the microfluidic channel walls [Fig. 3.3]. While 95% oxygen gas was flowing in one channel, in the adjacent channel 0% oxygen was flowing. The oxygen measurements taken show a steep change from one microfluidic channel to the adjacent one, while the Fura signal shows a similar change from one channel to the other. To further illustrate this point, we recorded the Fura response of the dentate gyrus and the CA1 area while each area was exposed to a different oxygen environment [Fig. 3.7]. Just like in the previous device, the CA1 was subjected to a hypoxic insult; however, this time the dentate gyrus was not exposed to the hypoxic condition. As expected, the CA1 area showed the distinct drop in Fura intensity signifying the increase in intracellular calcium, while the dentate gyrus did not suffer any change in calcium concentration. This clearly demonstrates the ability to deliver hypoxic stimuli with microscale precision and on time scales similar to *in vivo* stroke events.

As previously stated, with this device, we are able to stimulate different regions of the brain with different oxygen stimuli; however, in certain cases, a more refined stimulus may be necessary. With this in mind, we decided to design a way in which the oxygen stimulus could be concentrated to a limited space. In this case, we decided to use a number 1 coverslip to isolate the oxygen stimuli [Fig. 3.8]. We drilled a 1mm diameter hole into the coverslip and simply placed it inside the microfluidic device. By doing this, we are effectively blocking the oxygen diffusion into the aCSF or the brain slice, except for the area located where the drilled hole is. For this particular case, only the 1mm area can be stimulated while the rest of the slice remains unaffected. Using calcium imaging, we demonstrated that we could expose the 1mm area, which

we placed right on top of the CA1 area of the hippocampus, to a hypoxic response in much the same way that we did the different regions of the brain before.

4.2 –Future experiments

Until now, the lack of technology for localized deoxygenation prevented several ideas from being investigated *in vitro*. Stroke research is a prime candidate to take advantage of this technology where having the ability to control the oxygen environment of different brain regions independently of each other will lead to more insightful research into more relevant neuronal circuits. However, another area of interest could be obstructive sleep apnea, where it is known that intermittent hypoxia affects the hippocampus' role in learning and memory and where the CA1 and the dentate gyrus areas are affected differently (51, 52). Of course, the potential of this device is not limited to stroke research or neuroscience. Cyclic oxygenation is a common event throughout the body with muscle, kidney (47), and cancer cells (36) being an example. Advances in microfabrication technology allow us to optimize the microfluidic devices to fit the tissue and cells in question. The ability to control the oxygen environment in them will undoubtedly lead to better understanding of how cells react to changes in oxygen concentration.

CONCLUSION

How neuronal tissue responds to a hypoxic insult is a fundamental question to stroke research. In order to fully understand the relationship between oxygen and neuronal function, one should subject the tissue to an environment where the oxygen supply can be controlled both temporally and spatially without disturbing other variables.

Using our add-on microfluidic device, we can adjust the spatial oxygenation conditions inside the brain slice within a matter of minutes. With respect to previously used methods, the key advantages of our device include the minimal invasiveness of the procedure, the ability to maintain open access from above the chamber for electrophysiology tools, better temporal control over the hypoxic insult, and the ability to independently oxygenate different areas of the brain slice.

It is important to keep in mind that our device has many possible applications in neuroscience. Along with the ability to create a constant oxygen environment throughout the brain slice, we were able to subject the slice to hypoxic insults at controllable rates and at predetermined locations. As a proof of concept, we demonstrated that the device could deoxygenate the CA1 area of the hippocampus while keeping the dentate gyrus completely unaffected. Knowing that intracellular calcium increases during hypoxia in a neuron, we used the calcium indicator Fura-2 to measure the changes in calcium concentration and as expected, we determined that the device could completely isolate certain areas of the hippocampus. From our results, we determined that in order to obtain optimal results, a hypoxic area should have a radius of no less than 0.3mm, which is enough to separate the hippocampus into its different areas:

dentate gyrus, CA1 and CA3. For the next phase of the project, localized stimuli, we used a 1mm diameter hole to isolate the hypoxic insult and obtained favorable results.

We demonstrated that a microfluidic device that can be attached to a perfusion chamber is able to deliver a hypoxic stimulus to the cells all throughout the brain slice in a rapid and controlled manner. When compared to the perfusion method, our diffusion device allows complete spatial and temporal control over the oxygen environment with microscale precision, something that is not possible with any current methods. The ability to deliver localized oxygen stimuli to an *in vitro* model will undoubtedly motivate advances in stroke research, as well as in other tissues where cyclic oxygenation can provide further insight into the behavior of the body.

CITED LITERATURE

1. Wu, J.B., Song, N.N., Wei, X.B., Guan, H.S. and Zhang, X.M., Protective effects of paeonol on cultured rat hippocampal neurons against oxygen-glucose deprivation-induced injury. Journal of the Neurological Sciences, 2008. 264: p. 50-55.

2. Berdichevsky, Y., Sabolek, H., Levine, J.B., Staley, K.J. and Yarmush, M.L, Microfluidics and multielectrode array-compatible organotypic slice culture method. Journal of Neuroscience Methods, 2009. 178: p. 59-64.

3. Mulkey, D.K., Henderson, R.A., Olson, J.E., Putnam, R.W. and Dean, J.B., Oxygen measurements in brain stem slices exposed to normobaric hyperoxia and hyperbaric oxygen. Journal of Applied Physiology, 2001. 90: p. 1887-1899.

4. Cho, S., Wood, A. and Bowlby, M. R., Brain Slices as Models for Neurodegenerative Disease and Screening Platforms to Identify Novel Therapeutics. Current Neuropharmacology, 2007 5: p. 19-33.

5. Gähwiler, B.H., Capogna, M., Debanne, D., McKinney, R.A. and Thompson, S.M. , Organotypic slice cultures: A technique has come of age. Trends Neuroscience, 1997. 20(471-477).

6. Queval, A., Ghattamaneni, N.R., Perrault, C.M., Gill, R., Mirzaei, M., McKinney, R.A. and Juncker. D., Chamber and microfluidic probe for microperfusion of organotypic brain slices. Lab on a Chip, 2010. 10: p. 326-334.

7. Schurr, A., Brain slice preparation in electrophysiology. KOPF Carrier, 1986. October(15).

8. Tang, Y.T., Kim, J., Lopez-Valdes, H.E., Brennan, K.C. and Ju, Y.S., Development and characterization of a planar microfluidic device incorporating integrated fluid injection and suction ports for localized chemical stimulation of brain slices. Lab on a Chip, 2011. 11: p. 2247-2254.

9. Rambani, K., Vukasinovic, J., Glezer, A. and Potter, S.M., Culturing thick brain slices: an interstitial 3D microperfusion system for enhanced viability. Journal of Neuroscience Methods, 2009. 180: p. 243-254.

10. Medvedeva, Y.V., Lin, B., Shuttleworth, C.W. and Weiss, J.H. Intracellular Zinc accumulation contributes to synaptic failure, mitochondrial depolarization, and cell death in an acute slice oxygen-glucose deprivation model of ischemia. The Journal of Neuroscience, 2009. 29(4): p. 1105-1114.

11. Stork, C.J.a.L., Y.V., Rising zinc: a significant cause of ischemic neuronal death in the CA1 region of rat hippocampus. Journal of Cerebral Blood Flow and Metabolism, 2009. 29: p. 1399-1408.

12. Moser, M.B.a.M., E., Functional differentiation in the hippocampus. Hippocampus, 1998. 8: p. 608-619.

13. Tulving, E.a.M., H.J. , Episodic and declarative memory: Role of the hippocampus. Hippocampus, 1998. 8: p. 198-204.

14. Xue, J., Zhou, D., Yao, H. and Haddad, G.G., Role of transporters and ion channels in neuronal injury under hypoxia. Am. J. Physiol Regul Integr Comp Physiol, 2007. 294: p. 451-457.

15. Nitatori, T., Sate, N., Waguri, S., Karasawa, Y., Araki, H., Shibanai, K., Kominami, E., and Uchiyama, Y., Delayed Neuronal Death in the CA1 Pyramidal Cell Layer of the Gerbil Hippocampus following Transient lschemia Is Apoptosis. The Journal of Neuroscience, 1995. 15(2): p. 1001-1011.

16. Papazisis, G., Pourzitaki, C., Sardeli, C., Lallas, A., Amaniti, E. and Kouvelas, D., Deferoxamine decreases the excitatory amino acid levels and improves the histological outcome in the hippocampus of neonatal rats after hypoxia-ischemia. Pharmacological Research, 2008. 57: p. 73-78.

17. Hoffmann, U., Pomper, J., Graulich, J., Zeller, M., Schuchmann, S., Gabriel, S., Maier, R.F. and Heinemann, U., Changes of neuronal activity in areas CA1 and CA3 during anoxia and normoxic or hyperoxic reoxygenation in juvenile rat organotypic hippocampal slice cultures. Brain Research, 2006. 1069: p. 207-215.

18. Bickler, P.E.H., B.M. , Hypoxia-tolerant neonatal CA1 neurons: relationship of survival to evoked glutamate release and glutamate receptor-mediated calcium changes in hippocampal slices. Developmental Brain Research, 1998. 106: p. 57-69.

19. Bickler, P.E.H., B.M. , Causes of calcium accumulation in rat cortical brain slices during hypoxia and ischemia: role of ion channels and membrane damage. Brain Research, 1994. 665: p. 269-276.

20. Tonkikh, A.A., and Carlen, P.L., Impaired presynaptic cytosolic and mitochondrial calcium dynamics in aged compared to young adult hippocampal CA1 synapses ameliorated by calcium chelation. Neuroscience, 2009. 159: p. 1300-1308.

21. Bicker, P.E., Kelleher, J.A., Fructose-1,6-biphosphate stabilizes a brain intracellular calcium during hypoxia in rats. Stroke, 1992. 23(11): p. 1617-1622.

22. Cai, J., Kang, Z., Liu, W.W., Luo, X., Qiang, S., Zhang, J.H., Ohta, S., Sun, X., Xu, W., Tao, H. and Li, R., Hydrogen therapy reduces apoptosis in neonatal hypoxia-ischemia rat model. Neuroscience Letters, 2008. 441: p. 167-172.

23. Tian, L., Looger, L.L., Genetically encoded fluorescent sensors for studying healthy and diseased nervous systems. Drug Discovery Today: Disease Models, 2008. 5(1): p. 27-35.

24. Paula-Lima, A.C., De Felice, F.G., Brito-Moreira, J., and Ferreira. S.T., Activation of GABA receptors by taurine and muscimol blocks the neurotoxicity of B-amyloid in rat hippocampal and cortical neurons. Neuropharmacology, 2005. 49(1140-1148).

25. Cheran, L.E., Benvenuto, P., and Thompson, M., Coupling of neurons with biosensor devices for detection of the properties of neuronal populations. Chemical Society Reviews, 2008. 37: p. 1229-1242.

26. Rochefort, N.L., Jia, H. & Konnerth, A. Calcium imaging in the living brain: Prospects for molecular medicine. Trends. Mol. Med. **14**, 389-399 (2008).

27. Grynkiewicz, G., Poenie, M., and Tsien, R.Y, A new generation of Ca2+ indicators with greatly improved fluorescence properties. J.Biol.Chem, 1985. 260(6): p. 3440–3450.

28. Nakamura, I., Nakai, Y. & Izumi, H., Use of Fura-2/AM to Measure Intracellular Free Calcium in Selenomonas ruminantium. Tohoku J. Exp. Med, 1996. 179: p. 291-294.

29. Yuste R, L.F., Konnerth A, Imaging Neurons: A Laboratory Manual. C.S. Harbor. 2000, NY.: Cold Spring Harbor Laboratory Press.

30. Yuste, R., Konnerth, A., Imaging in neuroscience and development: A laboratory manual. Cold Spring Harbor 2005. NY. Cold Spring Harbor Laboratory Press.

31. Mohammed, J.S., Caicedo, H.H., Fall, C.P. and Eddington, D.T., Microfluidic add-on for standard electrophysilogy chambers. Lab on a Chip, 2008. 8: p. 1048-1055.

32. Hajos, N., Mody, I., Establishing a physiological environment for visualized in vitro brain slice recordings by increasing oxygen supply and modifying aCSF content. Journal of Neuroscience Methods, 2009. 183: p. 107-113.

33. Blake, A.J., Pearce, T.M., Rao, N.S., Johnson, S.M. and Williams J.C., Multilayer PDMS microfluidic cahmber for controlling brain slice microenvironment. Lab on a Chip, 2007. 7: p. 842-849.

34. Hajos, N., Ellender, T.J.,Zemankovics, R., Mann, E.O., Exley, R., Cragg, S.J., Freund T.F. and Paulsen, O., Maintaining network activity in submerged hippocampal slices: importance of oxygen supply. European Journal of Neuroscience, 2009. 29: p. 319-327.

35. D. Bingmann, G.K., PO2 profiles in hippocampal slices of the guinea pig. Experimental Brain Research, 1982. 48: p. 89-86.

36. Oppegard, S.C., Nam, K.H., Carr, J.R., Skaalure, S.C. and Eddington, D.T., Modulating temporal and spatial oxygenation over adherent cellular cultures. PLOS One, 2009. 4(9): p. 1-6.

37. Pomper, J.K., Graulich, J., Kovacs, R., Hoffmann, U., Gabriel, S. and Heinemann, U., High oxygen tension leads to acute cell death in organotypic hippocampal slice cultures. Developmental Brain Research, 2001. 126: p. 109-116.

38. Sakadzic, S., Roussakis, E., Yaseen, M.A., Manderville, E.T., Srinivasan, V.J., Arai, K., Ruvinskaya, S., Devor, A., Lo, E.H., Vinogradeov, S.A. and Boas, D.A., Two-photon high-resolution measurement of partial pressure of oxygen in cerebral vasculature and tissue. Nature Methods, 2010: p. 1-7.

39. Turner, D.A.F., K.A., Galeffi, F. and Somjen, G.G., Differences in O2 availability resolve the apparent discrepancies in metabolic intrinsic optical signals in vivo and in vitro. Trends in Neuroscience, 2007. 30(8): p. 390-396.

40. Jessamine M. K., G., I., Stroock, A.D. and Whitesides, G.M., Components for integrated poly(dimethylsiloxane) microfluidic systems. Electrophoresis, 2002. 23: p. 3461-3473.

41. Whitesides, G.M., Ostuni, E., Takayama, S., Jiang, X. and Ingber, D.E., Soft lithography in biology and biochemistry. Annu. Rev. Biomed. Eng., 2001. 3: p. 335-373.

42. Mehta, G., Mehta, K., Sud, D., Song, J.W., Bersano-Begey, T., Futani, N., Heo, Y.S., Mycek, M.A., Linderman, J.J. and Takayama, S., Quantitative measurement and control of oxygen levels in microfluidic poly(dimethylsiloxane) bioreactors during cell culture. Biomed Microdevices, 2007. 9: p. 123-134.

43. Lam, R.H.W., Kim, M.C., and Thorsen, T., Culturing aerobic and anaerobic bacteria and mammalian cells with a microfluidic differental oxygenator. Anal. Chem., 2009. 81(14): p. 5918-5924.

44. Xia, Y., Whitesides, G.M., Soft lithography. Annu. Rev. Mater sci., 1998. 28: p. 153-184.

45. Anderson, J.R., Chiu, D.T., Jackman, R.J., Cherniavskaya, O., McDonald, J.C., Wu, H., Whitesides, S.H. and Whitesides, G.M., Fabrication of topologically complex three-dimensional microfluidic systems in PDMS by rapid prototyping. Anal. Chem., 2000. 72: p. 3158-3164.

46. Beierlein M, F.C., Rinzel J, Yuste R, Thalamocortical bursts trigger recurrent activity in neocortical networks: layer 4 as a frequency-dependent gate. T J Neurosci, 2002. 22(22): p. 9885-9894.

47. Lo, J.F., Sinkala, E. & Eddington, D.T., Oxygen Gradients for Open Well Cellular Cultures via Microfluidic Substrates. Lab on a Chip, 2010. 10(18): p. 2394-2401.

48. Nolan, P.C.W., T.G. , Ventrolateral medullary neurons show age-dependent depolarizations to hypoxia in vitro. Developmental Brain Research, 1996. 91: p. 111-120.

49. Choi, Y., McClain, M.A., LaPlaca, M.C., Frazier, A.B. and Allen, M.G., Three

dimensional MEMS microfluidic perfusion sytem for thick brain slice cultures. Biomed Microdevices, 2007. 9: p. 7-13.

50. Passeraub, A., Almeida, A.C. & Thakor, N.V. , Design, Microfabrication and Analysis of a Microfluidic Chamber for the Perfusion of Brain Tissue Slices. Biomedical Microdevices, 2003. 5(2): p. 147-155.

51. Aleisa, A., Helal, G., Alhaider, I., Alzoubi, K., Srivareerat, M., Tran, T., Al-Rejaie, S. and Alkadhi, K., Acute nicotine treatment prevents REM sleep deprivation-induced learning and memory impairment in rat. Hippocampus, 2011(21).

52. Hambrecht VS, V.P., Row BW, Gozal D, Baghdoyan HA, Lydic R. , Hypoxia modulates cholinergic but not opioid activation of G proteins in rat hippocampus. Hippocampus, 2007. 17(10): p. 934-942.

VITA

Gerardo Mauleon

EDUCATION

2009-2011 **Master of Science in Bioengineering**
University of Illinois at Chicago
Advisor: Dr. David T. Eddington
Thesis: Stroke on a Chip: Spatial and Temporal Control of Oxygen for *in vitro* Brain Slices
Synopsis: Designed, fabricated, validated, and utilized a microfluidic device that allows greater spatial and temporal control over the oxygen environment experienced by acute brain slices and studied the relationship between hypoxia and intracellular calcium.

2005-2009 **Bachelor of Science in Bioengineering**
University of Illinois at Chicago

RELEVANT SKILLS

Microfabrication
- Soft lithography and photolithography
- PDMS microfluidic devices
- Computational fluid dynamics (COMSOL multiphysics software)

Cell biology
- Animal handling and surgical procedures
- Brain tissue slices and staining
- Fluorescence microscopy

CONFERENCE PROCEEDINGS

Poster Presentations

- UIC Student Research Conference - Chicago, IL (March 2011)
  Title: "Stroke on a Chip: Spatial and Temporal Control of Oxygen for *in vitro* Brain Slices."

HONORS AND ACTIVITIES

Presidential Award
Transfer Merit Scholarship
Honor's College tuition waiver scholarship
UIC Department Award Scholarship
Square D-Engineering Scholarship

PROFESSIONAL SOCIETIES

Phi Theta Kappa - Honor Society of the Two Year College
Honor's College - UIC
Society of Hispanic Professional Engineers
Tau Sigma Honor Society
Alpha Eta Mu Beta - National Biomedical Engineering Honor Society
Tau Beta Pi - Engineering Honor Society